BEHAVIOUR OF CARBON BLACK NANO-ENGINEERED CEMENTITIOUS COMPOSITE AT ELEVATED TEMPERATURE

A Dissertation Submitted in Partial Fulfilment of the Requirement

For the Degree of

MASTER OF ENGINEERING

STRUCTURAL ENGINEERING

Submitted by

NITISH KUMAR

802124012

Under the guidance of

Dr. A.B Danie Roy

(Assistant Professor.)

CED, T.I.E.T, PATIALA.

Dr. Arpit Goyal

(Assistant Professor.)

CED, T.I.E.T, PATIALA.

THAPAR INSTITUTE
OF ENGINEERING & TECHNOLOGY
(Deemed to be University)

CIVIL ENGINEERING DEPARTMENT

THAPAR INSTITUTE OF ENGINEERING & TECHNOLOGY

(DEEMED TO BE UNIVERSITY), PATIALA, PUNJAB

JULY 2023

ACKNOWLEDGEMENT

I extend my sincere gratitude to **Dr. A.B Danie Roy** Assistant Professor at TIET, Patiala, and **Dr. Arpit Goyal**, Assistant Professor at TIET, Patiala, for their unwavering guidance, support, and patience. Their willingness to listen to my ideas and provide valuable suggestions for implementation has been invaluable throughout my work. Their constant motivation and inspiration have been instrumental in my journey.

I am deeply thankful to **Akshay Sharma**, a Ph.D. student in the Civil Engineering Department at TIET, for his valuable suggestions and timely cooperation in operating the Electric Furnace. His assistance played a crucial role in successfully carrying out this dissertation.

I am also grateful to the entire academic community and staff at TIET for creating an enriching environment that fostered learning and growth. Their contributions have significantly contributed to the completion of this research.

Lastly, I would like to express my heartfelt thanks to my family and friends for their unwavering support and encouragement throughout this academic endeavor. Their belief in my abilities has been a constant source of strength and motivation.

Date:- 28-07-2023

NITISH KUMAR
802124012

DECLARATION

I hereby declare that this is a bonafide work which is presented in this dissertation entitled **'BEHAVIOUR OF CARBON BLACK NANO-ENGINEERED CEMENTIOUS COMPOSITE AT ELEVATED TEMPERATURE'** as per the requirements for the award of Master of Engineering in Structural Engineering, submitted in the Department of Civil Engineering, Thapar Institute of Engineering and Technology (TIET), Patiala. This work is carried out under the guidance of Dr. Danie Roy A.B. and Dr. Arpit Goyal. It is declared that the work is original and has not been submitted anywhere else for the award of any degree or certificate.

Date - 6-09-2023

Nitish Kumar

This is to certify that the above declaration made by the concerned student is correct and true to the best of my knowledge and belief.

Dr. A.B Danie Roy
(Assistant Professor)
CED, TIET, Patiala.

Dr. Arpit Goyal
(Assistant Professor)
CED, TIET, Patiala.

Date : 6/9/23.

Abstract

Nanomaterials have introduced fundamental changes in cement-based composites at sub-microscale and microscale levels, resulting in modifications in molecular structures. These nanoscale alterations significantly influence the macroscale properties of the composites. Nanotechnology's distinctive attributes, such as substantial surface area and enhanced hydration rate, have led to remarkable mechanical strength and durability enhancements. Carbon black, a fine particle of elemental carbon, is known for its high conductivity, UV resistance, and pigmenting abilities. It finds various applications in industries, including rubber, where it reinforces tires and rubber products for improved strength and wear resistance.

Including carbon black nanoparticles in cementitious composites has gained attention for its positive impact on mechanical properties. Carbon black's high surface area-to-volume ratio allows enhanced reactivity and filling of pores and microcracks in the cement matrix, leading to improved densification and hydration processes. This research investigates the effects of increased temperature on key properties of nanoengineered composite mortar, focusing on compressive strength, flexural strength, mass loss, and colour change.

Results demonstrate that carbon black nanoparticles effectively replace cement in nanoengineered composite mortar, showing favourable properties in fresh and hardened states. The observed strength reduction due to temperature variations is effectively mitigated by incorporating 2% carbon black. Microstructural analysis reveals alterations resulting from carbon black substitution and temperature effects. These findings highlight the potential of utilizing carbon black nanoparticles as a cement alternative in the construction industry, leading to improved nanoengineered composite mortar with enhanced fire resistance properties.

This research demonstrates nanomaterials' potential to enhance cement-based composites, improving performance in diverse temperature conditions. It highlights nanotechnology's significant role in advancing construction materials, promising more durable and resilient cementitious composites, revolutionizing the industry.

KEYWORDS – Carbon Black, Elevated Temperature, Mortar, Nanoengineered composites, Slump Flow

TABLE OF CONTENT

LIST OF FIGURES

LIST OF TABLES

LIST OF ABBREVATIONS

C–S–H	calcium-silicate-hydrates
CH	calcium hydroxide (portlandite)
ITZ	interfacial transition zone
OPC	Ordinary Portland cement
HSC	High strength concrete
CNT	carbon nanotube
MWCNT	multi-walled carbon nanotube
SWCNT	Single Wall Carbon Nanotube
GNP	Graphene Nanoplatelets
GO	Graphene oxide
rGO	Reduced Graphene Oxide
CBN	Carbon Black Nanoparticles
MIP	Mercury intrusion porosimeter
XRD	X-ray diffraction
FESEM	Field Emission Scanning Electron Microscopy
SP	Super Plasticizer

Chapter 1
INTRODUCTION

1.1 General

Cement-based composites are extensively utilized in construction, yet they face considerable challenges when exposed to high temperatures, like fire disasters and nuclear power plant accidents, leading to compromised mechanical properties and durability. Researchers have diligently investigated the impact of elevated temperatures on these composites and sought solutions to enhance their fire resistance. The degradation in the characteristics of cement-based composites at elevated temperatures is thought to be the dehydration and breakdown of the cement hydration products predominantly, calcium silicate hydrate (C-S-H) and calcium hydroxide (CH) micro- and nanoscale behaviors in governing the mechanical performance of these materials. (Alhamad et al., 2022; Malik et al., 2021; Pulkit & Adhikary, 2022). In general circumstances, Ordinary Portland Cement (OPC) exhibits adequate strength to withstand fire. It is commonly employed as a protective covering for reinforcement in fire-resistant applications. Nevertheless, exposure to elevated temperatures induces notable physical and chemical changes in OPC, resulting in a decline in its mechanical properties. The hydration reaction of OPC generates Calcium hydroxide ($CaOH_2$), contributing to its strength. However, $CaOH_2$ decomposes at temperatures of approximately 400 °C, yielding water and calcium oxide (CaO). Beyond this threshold, a complete loss of strength occurs due to the dehydration and dissociation of $CaOH_2$, coupled with the rehydration of CaO. Furthermore, the strength-giving compound, Calcium-silicate-hydrate gel (CSH), experiences additional decomposition when subjected to temperatures exceeding 600 °C, ultimately leading to the typical disintegration of concrete around 800 °C

Conventional reinforcement techniques, operating at the macroscopic scale, have involved the use of aggregates, fibers, and supplementary cementitious materials. However, recent findings highlight the pivotal role of microscopic and nanotechnology in materials. The quest for new materials with enhanced properties at higher temperatures is of utmost significance. Nano-cementitious composites emerge as a promising alternative to traditional cement, offering potential as new cementing materials. Carbon

black nanoparticles utilize waste materials and hold promise for environmentally sustainable construction practices. This study highlights the importance of seeking innovative solutions to address the challenges posed by elevated temperatures in construction materials.

1.1 Nanomaterial Incorporation in Construction

In recent years, the application of nanotechnology has emerged as a promising and innovative approach to enhancing the fire resistance of cement-based composites. By introducing nanomaterials into these composites, fundamental alterations occur at both the sub-microscale and microscale levels, leading to modifications in molecular structures. These nanoscale changes have a significant impact on the overall macroscale properties of the cement-based composites, imparting improved fire resistance.

The properties exhibited by cement-based materials at various length scales, ranging from nano to micro to macro structures, are inherently dependent on the behaviors and characteristics observed at the smaller scale. This underscores the multiscale nature of cement-based composites and their response to nanomaterial incorporation for enhanced fire resistance. Significant progress has been made in the comprehension and application of nanomaterials within this domain. The distinctive attributes of nanomaterials, including their substantial surface area and ability to enhance the hydration rate, have resulted in remarkable enhancements in the mechanical strength and durability of cement-based composites. These advancements signify the substantial contributions of nanotechnology in this field and its potential to revolutionize construction materials(Pehlivan et al., 2023; Singh et al., 2019)

The rapid advancement of nanotechnology and nanomaterials has opened up promising avenues for enhancing cementitious composites at the nanoscale. Even when introduced at very low concentrations, nanomaterials can remarkably influence cement-based materials' performance, encompassing aspects like mechanical strength, chemical resistance, and transport capabilities. By incorporating nanomaterials as fillers or partial substitutes for binders in cement concrete, the flow characteristics and morphology at the nanoscale can be modified, leading to substantial improvements in the mechanical and durability properties of cementitious composites. A comprehensive investigation of carbon-based nanomaterials has unveiled their positive impact on cement composites.

Among the extensively studied carbon-based nanomaterials are carbon nanotubes (CNT), graphene nanoplatelets (GNP), graphene oxide (GO), reduced graphene oxide (rgo), and nanocarbon black (CBN). These materials have shown great promise in elevating the overall performance of cementitious composites due to their exceptional properties at the nanoscale. Integrating nanotechnology and nanomaterials holds significant potential in revolutionizing the construction industry, offering sustainable solutions for developing high-performance, durable, and environmentally friendly cement-based materials.

Further research and exploration of these nanomaterials are crucial to unlock their full potential and pave the way for the construction of advanced infrastructure with enhanced properties and increased resilience against diverse challenges. The application of nanomaterials in cement composites can contribute significantly to the sustainable development of the construction sector, reducing resource consumption, improving infrastructure durability, and minimizing environmental impacts. However, it is essential to note that as this field progresses, comprehensive investigations into the potential health and environmental impacts of nanomaterials should be conducted to ensure their safe and responsible usage in construction applications. Overall, the ongoing headway in microstructure advancements through nanotechnology offers a promising pathway toward innovation in cementitious composites, fostering a greener and more resilient built environment.

1.2 Different Types of Carbon-Based Nano Composites

1.2.1 Graphene Nano Platelets

A stable allotrope of carbon called graphite is normally found in quartz and limestone ore deposits. A particular sheet of this structure is called graphene. Multiple layers of graphene sheets stacked on best of one another Figure 1.1(a) make multilayer graphene (MLG), known as graphene Nanoplatelets (GNP). GNP is well recognized for its vast surface area properties and high aspect ratio. Their thickness ranges from a few to dozens of nanometres, usually measured at the nanoscale GNP has been synthesized using numerous techniques, namely arc discharge and chemical vapour deposition (CVD).

The wrinkled network architecture of GNPs is visible in the image Figure 1.1(b) from scanning electron microscopy, which supports the filling action of GNPs in a cement matrix. Their poor dispersion in aqueous solutions in fluid arrangements is one of the main barriers to GNP in cement-based composites. Due to the hydrophobic properties of

GNPs, the high surface energies of nanoparticles, strong van der Waal forces, and other factors make it challenging to create a homogeneous solution. Which tends to make agglomerate in water. The foremost popular method for dispersing GNPs into cementitious composites has been ultrasonic treatment combined with mechanical agitation and surfactants (Afzal et al., 2016; Liu et al., 2019; Yakovlev et al., 2006)

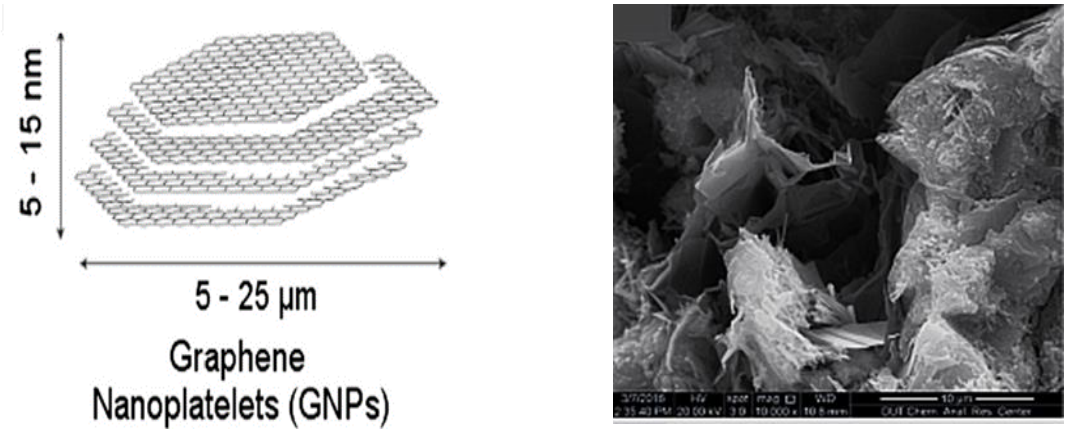

a)GNP Schematic (Shamsaei et al., 2018) b)SEM of GNP (Wang & Shuang, 2018)

Figure 1.1 a) GNP Schematic and b) SEM image

1.2.2 Carbon Nano Tubes

Carbon nanotube was founded by Iijima in 1991. Graphene is a 2D single sheet of graphite included in the carbon nanomaterials group. Carbon atoms are arranged in a graphene hexagonal pattern, as shown in Figure 1.2(a). Carbon nanotubes are created when these graphene sheets are rolled up into a cylinder (CNTs). CNTs are round and hollow-shaped carbon allotropes which can be categorized into two primary bunches of single-walled carbon nanotubes (SWCNTs) and multi-walled carbon nanotubes (MWCNTs), as demonstrated in Figure 1.2(b-c)

CNTs can be the optimum filler for the next generation of high-performance and versatile cementitious composites. Dispersion of CNT in cement composites by surfactant-assisted ultra-sonication is considered the most popular and best-fitted technique out of others that are available. After the dispersion, good availability of CNTs in cement composites makes higher density C-S-H gel structure and a more confined interfacial transition zone between the aggregates in the cement matrix, which may offer more nucleation sites to speed up the hydration process. The finely tuned pore structure created by CNTs lowers

the capillary tension. This reduces permeability and improves structural strength, reducing autogenous shrinkage, pores distribution and increasing durability. Due to dispersion difficulties, CNTs at a high reinforcement ratio may reduce the mechanical and durability qualities (Ramezani et al., 2022; Rathinavel et al., 2021)

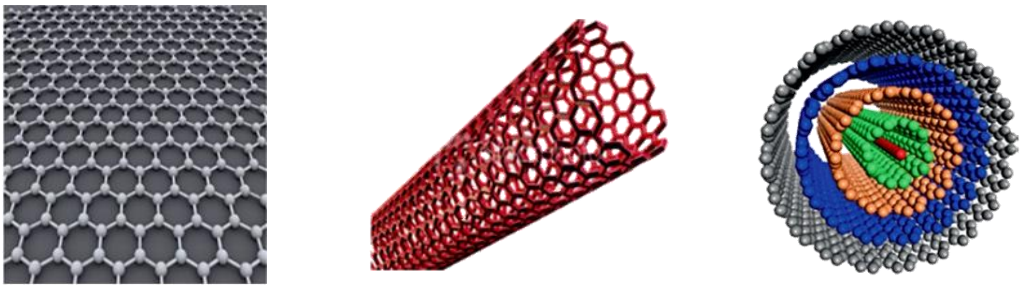

a) Carbon atom arrangement in Graphene

b) SWCNT)

c) MWCNT

Figure 1.2 CNT Schematic ((Kaushik & Majumder, 2015)

1.2.3 Graphene Oxide

Graphene oxide (GO) is a carbon-based nanomaterial with dimensions below 100 nm, featuring a layered carbon structure covalently bonded with oxygen-containing functional groups like hydroxyl (-OH), epoxides (-O-), carboxyl (-COOH), and ketone carbonyls (-COO) (Kumar et al., 2016) This aromatic monolayer structure, as depicted in Figure 1.3 has been created by Benjamin C. Brodie. Studies suggest that GO is a promising choice for enhancing cement-based composites, leading to improved characteristics. During cement hydration, GO exhibits a flower-like structure, contributing to the enhancement of the cement matrix. Oxygen-bearing functional groups facilitate homogenous dispersion, C-S-H nucleation, and microstructure densification in cement. The strong reactivity of GO enhances cement hydration by providing attachment sites for C-S-H gel formation, thereby positively impacting the overall performance of cement-based materials (Alhamad et al., 2022).

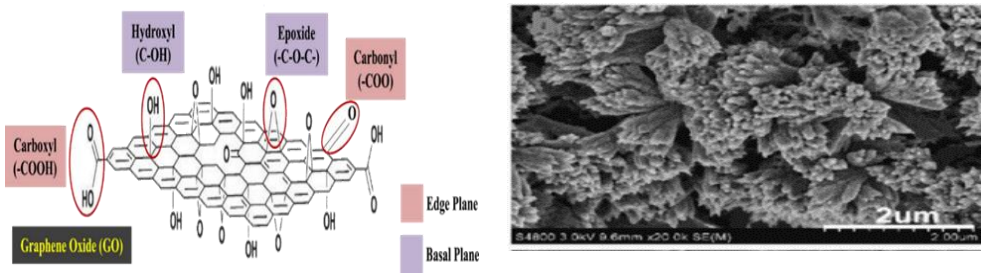

a) b)

Figure 1.3 a) GO Schematic and b) SEM image (Anwar et al., 2023)

1.2.4 Reduced Graphene Oxide

Reduced Graphene oxide rGO is a by-product of GO chemical or thermal reduction. The reduction of GO, functional groups, is mainly done by thermal or depends on the type of applications for the concrete design. As seen in Figure 1.4(a) shows that the reduced functional group of rgo gives it a hydrophobic property, leading to increased final setting time and workability characteristics. rGO addition led to narrow non-uniform platelets and a non-entangled network of rod-like crystals in Figure 1.4(b). This helps the rGO to give a characteristic to be a reasonable alternative to graphene sheets such as GO, with applications providing reduced aggregation in cement composites. Though rGO incorporation in cement composites is a new research direction, the durability and strength aspects could be more evident. (Chintalapudi & Pannem, 2020; Qureshi & Panesar, 2020)

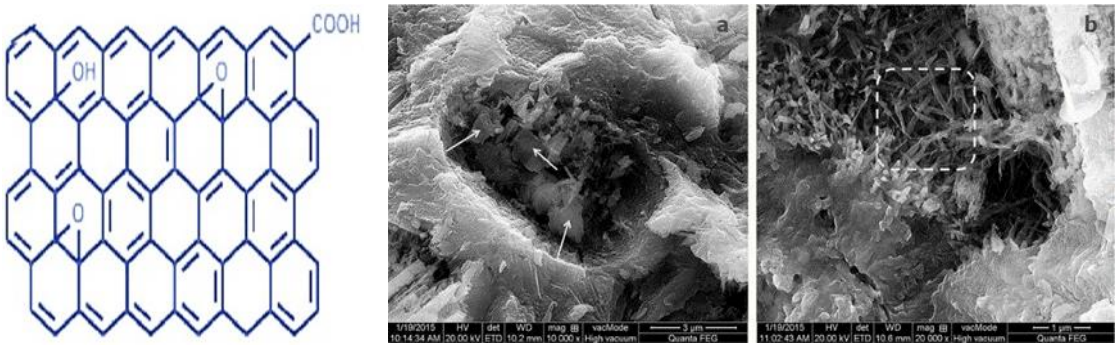

a) b)

Figure 1.4 a) rGO Schematic and b) SEM arrangement (Chintalapudi & Pannem, 2020)

1.2.5 Carbon Black

Carbon black is the general term for a family of small carbon nanoparticles during the thermal decomposition of hydrocarbons. Due to the temperature gradient caused by various oxygen depletions, oil drops or gaseous hydrocarbons are incompletely burned during the combustion of fuel oils. CBN are less than 300 nm in size(Bera et al., 2019). Carbon black shows good behaviour in self-sensing concrete for civil engineering infrastructures. Carbon Black is acceptable as a conductive filler in the manufacture of multifunctional cement composites. Scanning Electron Microscopic images shows that carbon black has a bead-like porous structure, as shown in Figure 1.5. With an increase in Carbon black content, compressive strength also increases reported in these studies (Dai et al., 2010) (Afzal et al., 2016)

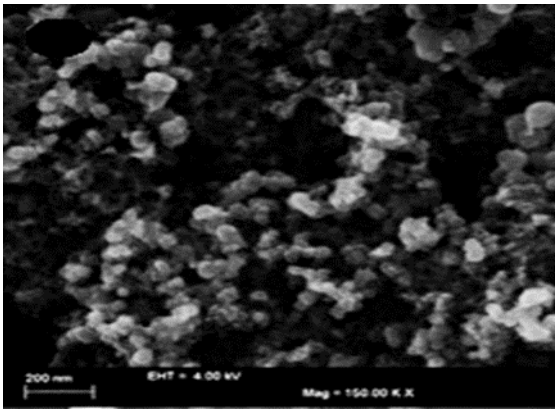

Figure 1.5 SEM image of CB (Afzal et al., 2016)

1.3 Ordinary Materials in Construction

Cement mortar is an indispensable binding material widely utilized in civil engineering construction due to its crucial role in facilitating structural integrity. Preparing cement mortar involves carefully amalgamation of water, cement, and sand to achieve a homogenous mixture. This composite is a critical adhesive agent, firmly uniting essential building blocks, such as bricks and concrete elements, during construction projects. Beyond its primary function as a binding agent, cement mortar serves an additional vital purpose in construction. It proficiently fills the pores within the concrete matrix, acting as a cohesive paste that effectively binds diverse materials together, reinforcing the overall structural integrity.

Moreover, the versatile nature of cement mortar extends its utility to various construction tasks, including plastering and surface finishing, thereby contributing to the aesthetics and durability of constructed structures. By meticulously enhancing the characteristics of the mortar mix, the overall quality and performance of the concrete are significantly improved. Notably, the water-to-cement ratio in mortar generally surpasses that found in concrete, allowing for optimal workability and application in different construction scenarios. The judicious application of cement mortar in civil engineering projects underscores its pivotal role in ensuring constructed structures' stability, strength, and longevity, rendering it an indispensable component of modern construction practices.

Chapter 2

Literature Review

2.1 General

Nanocomposites are a class of innovative materials wherein at least one constituent exhibits dimensions ranging from 1 to less than 100 nm (Kostoff et al., 2007) The enhanced physical and chemical properties of nanocomposites, surpassing those of traditional composites, can be attributed to the surface effect, small size effect, and tunnel effect arising from the quantum size phenomena of nanofillers at the nanoscale. Nanocarbon materials (NCMs) have garnered significant attention owing to their remarkable mechanical attributes, low density, and exceptional thermal and chemical stability. Among the emerging materials in the 21st century, nano-cementitious composites are rapidly gaining recognition as highly promising (C. Huang & Cheng, 2017) The categorization of nanoparticles can be based on diverse characteristics such as shape, size, morphology, and properties. Accordingly, nanofillers can be classified into three distinct groups: nanoplatelets (one nanoscale dimension), nanofibers (two nanoscale dimensions), and nanoparticles (three nanoscale dimensions). Notably, nanometric silica particles are encompassed within the classification of three-dimensional nanofillers. An overview study on the different carbon-based nanomaterials shows that incorporating minute quantities of nanocomposites into cement mortars led to the uniform dispersion of the nanocomposite materials. Consequently, the addition of these nanocomposites resulted in notable enhancements in the mechanical properties of the cement mortars, particularly in terms of compressive strength and hardness, when compared to the plain/reference sample (Huang. C & Cheng, 2017) The utilization of nanomaterials in concrete is gaining traction within the construction industry. The dense nanomaterial structure leads to enhancement in the corrosion resistance against the steel reinforcement, consequently extending the durability and lifespan of buildings.

2.2 Systematic overview

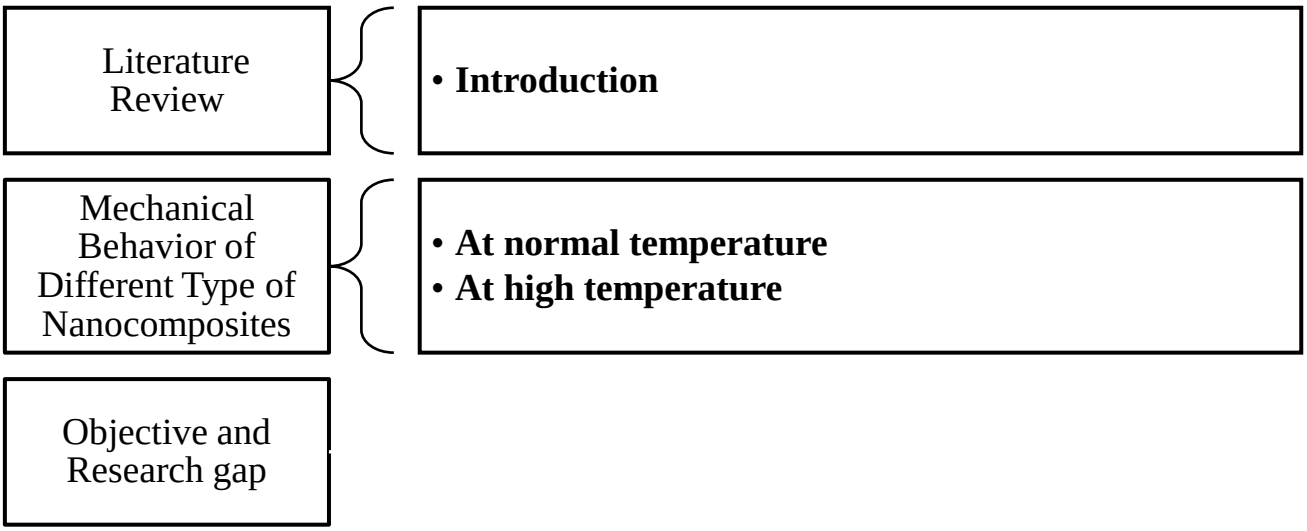

2.3 Mechanical Behaviour of Various Carbon-Based Nano-Cementious Composites at Normal Temperature.

2.3.1 Graphene Nano platelets –

(Ismail et al., 2022) investigated the influence of graphene Nanoplatelets (GnP) on the structural properties of reinforced concrete mortar (GnP-RC) beams and cylinders. The specimens had dimensions of 100 ×100 ×500 mm for beams and 150 mm diameter × 300 mm for cylinders, and GnP concentrations ranging from 0.00% to 0.50% by weight of cement were studied. The compressive strength test revealed that GnP had a controlling effect on reducing crack width Figure 2.1 through the nucleating action of the Nano filler in the cement matrix. The study also assessed the mechanical performance of GnP-RC samples and observed improvements in compressive, tensile, and flexural strengths. Notably, at a GnP content of 0.02%, the compressive strength increased by 20.82%, tensile strength by 30.05%, and flexural strength by 13.16% Figure 2.2 These findings suggest that incorporating GNP into cementitious composites holds potential as a method for extending the service life of structural elements.

Figure 2.1 Crack width in Specimens with respect to GNP % (Ismail et al. 2022)

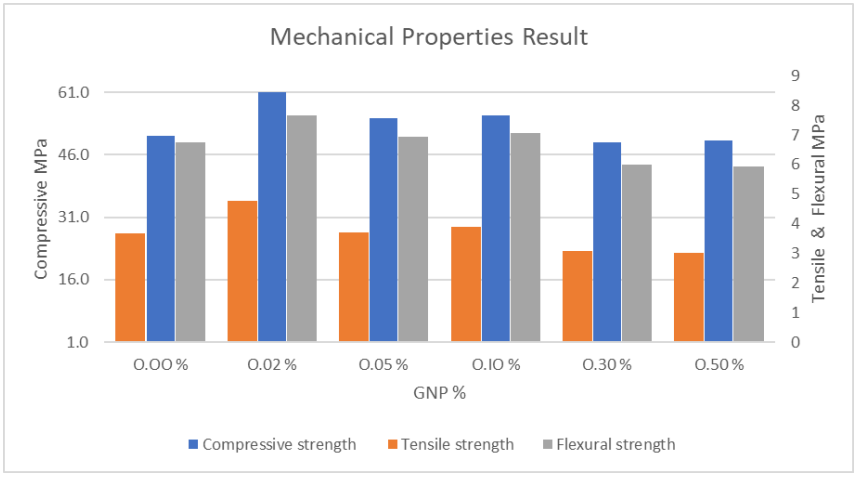

Figure 2.2 Mechanical Properties Results (Ismail et al., 2022)

(Sevim et al., 2022) examined the effects of nine types of graphene Nanoplatelets (GNP) with varying surface and size properties on mortar composites. GNP concentrations of 2.5%, 5%, and 7.5% by weight of cement were used. The study found that the highest compressive strength was achieved with a GNP concentration of 2.5% while increasing the concentration led to a substantial reduction in compressive strength. This reduction was attributed to improper mixing of GNP with cement, resulting in agglomerates and a more porous concrete structure. The study emphasized the significant role of GNP's physical properties, particularly its small thickness, in enhancing the strength properties of the concrete.

(Sevim et al., 2022) This study aimed to investigate the effects of graphene nanoplatelets (GNPs) on the mechanical properties of coarse aggregate in concrete. Different concentrations of GNPs (0%, 0.25%, 0.75%, and 0.10%) and dispersion methods (high

shearing and ultrasonication) were employed. Flexural and compressive strength tests were conducted using cylindrical specimens (76.2 × 76.2 × 279.4 mm and Φ101.6 × 203.2 mm)

Table 2-1 Dispersion Methods and (Jiang, Sevim, and Ozbulut 2021

Dispersion case	High-shear mixing	Ultrasonication	Exponenantial Data (Average Flake size)
H1	30 min	0	14.4 um
H2	60 min	0	11.2 um
H3	90 min	0	11.4 um
HU1	30 min	15 min	9.6 um
HU2	60 min	15 min	8.2 um
HU3	90 min	15 min	4.7 um

The results indicated that the compressive strength significantly improved with 60 minutes of high shear mixing and 15 minutes of ultrasonication at a low % GNP dosage of 0.05%. The researchers concluded that proper mixing of GNPs at lower concentrations contributed to the densification of the cement matrix, as evident in the SEM image of the 0.05% dosage., (Sevim et al., 2022) examined the effects of nine types of graphene Nanoplatelets (GNP) with varying surface and size properties on mortar composites. GNP concentrations of 2.5%, 5%, and 7.5% by weight of cement were used. The study found that the highest compressive strength was achieved with a GNP concentration of 2.5% while increasing the concentration led to a substantial reduction in compressive strength. This reduction was attributed to improper mixing of GNP with cement, resulting in agglomerates and a more porous concrete structure. The study emphasized the significant role of GNP's physical properties, particularly its small thickness, in enhancing the strength properties of the concrete.

(Sevim et al., 2022) This study aimed to investigate the effects of graphene nanoplatelets (GNPs) on the mechanical properties of coarse aggregate in concrete. Different concentrations of GNPs (0%, 0.25%, 0.75%, and 0.10%) and dispersion methods (high shearing and ultrasonication) were employed. Flexural and compressive strength tests were conducted using cylindrical specimens (76.2 × 76.2 × 279.4 mm and Φ101.6 × 203.2 mm)

Table 2-1 also demonstrated that the smallest graphene sheets were produced when ultrasonication and 15 minutes of shear mixing were employed.

The study highlights the significant influence of GNP size and dispersion methods on the mechanical strength of concrete. The findings suggest that the optimal dosage range and effective dispersion can enhance the mechanical properties of concrete composites.

(Baomin & Shuang, 2019) investigated the influence of Graphene Nano Platelets (GNPs) on cement composites' hydration reaction. Different concentrations of GNPs (0.03%, 0.06%, and 0.09% by weight of cement) were studied, and the optimal percentage was found to be 0.06% for achieving the highest compressive and flexural strength. Scanning electron microscopy (SEM) analysis in Figure 2.3 revealed that the inclusion of GNPs accelerated hydration and promoted the generation of more hydration products. This was attributed to enhanced ion exchange facilitated by GNPs, resulting in a denser microstructure and improved mechanical properties of the cement composites. The study highlights the potential of GNPs as a promising additive for enhancing cement composites' mechanical performance.

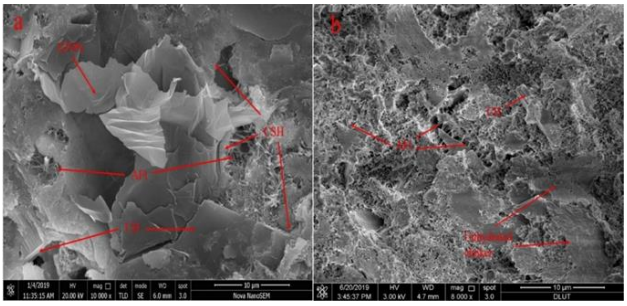

Figure 2.3 SEM Images of 0.06% & REF. Sample (Baomin and Shuang 2019)

(Tao et al., 2019) investigated the influence of Graphene Nano Platelets (GNPs) on the piezoresistive properties of cement mortars. Different concentrations of GNPs (ranging from 0% to 1% by weight of cement) were examined in Figure 2.4 with an optimal dosage of 0.05%, resulting in an 8.28% increase in compressive strength and a 15.6% increase in flexural strength. SEM analysis in Figure 2.5 demonstrated that well-dispersed GNPs within the cement matrix led to a more uniform distribution of cement hydrates, inhibiting flaws and crack formation. The study suggests that the incorporation of nano additives like GNPs alters the traditional mechanism of strength improvement by reducing porosity in cement-based materials (CBMs).

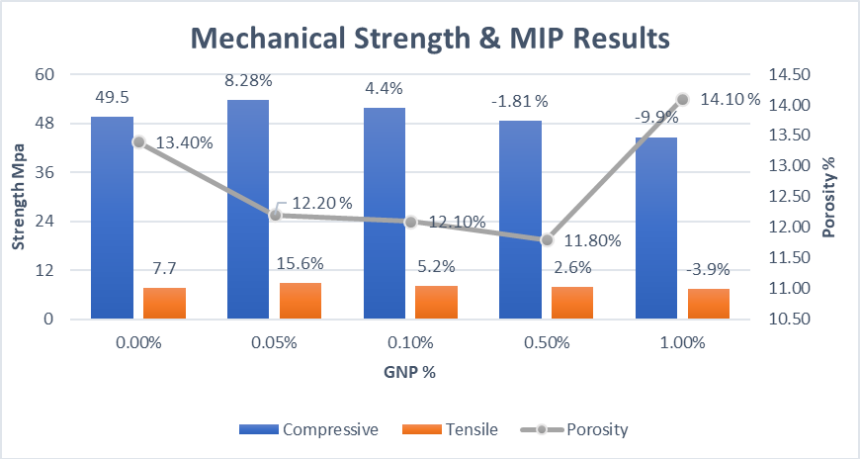

Figure 2.4 Mechanical & MIP Results (Tao et al. 2019)

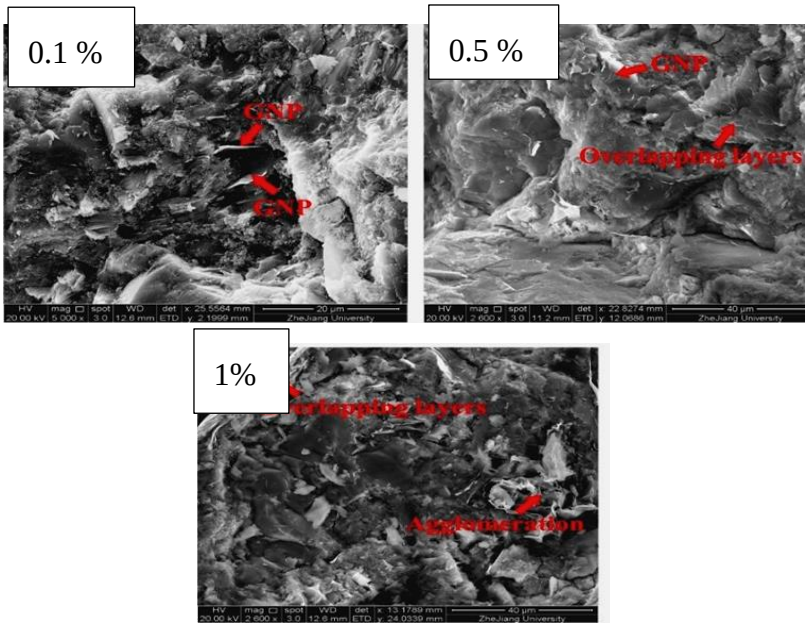

Figure 2.5 SEM Images with presence GNP mixes at different % (Tao et al. 2019)

(Chen et al., 2022) investigated concrete durability with varying GNP contents (0%, 0.02%, 0.05%, 0.1%, 0.2%, 0.3%, and 0.4%) subjected to freeze-thaw cycles. An optimal GNP content of 0.05% demonstrated the least compressive strength loss and lowest mass loss ratio. SEM analysis revealed a reinforced microstructure with reduced crack sizes, suggesting that incorporating graphene nanoplatelets can enhance concrete durability under freezing-thawing conditions.

(Wang & Shuang, 2018) investigated the impact of graphene nanoplatelets (GNPs) on cement-based materials. GNPs were dispersed in mixing water using a dispersant and ultrasonication at various concentrations (0.02% to 0.10% by weight of cement). The

study observed significant improvements in compressive and flexural strength in the GNP/cement composites, with an optimal concentration of 0.05%. Microstructural analysis indicated a reduction in total porosity by 40.80%, leading to a more compact and dense structure. Scanning electron microscopy (SEM) images showed enhanced alignment of calcium hydroxide (CH) structures, suggesting the role of GNPs as fillers and nucleating agents. Overall, GNPs' incorporation enhanced the mechanical strength of cement composites.

(Wang, Jiang, and Wu 2016) investigated the mechanical behavior of cement paste incorporating graphene nanoplatelets (GNPs) at a 0.05% concentration by weight of cement. Flexural and compressive tests on specimens demonstrated significant improvements in flexural strength (15%-24%) and compressive strength (3%-8%) at various intervals. Microstructural analysis in Figure 2.6 revealed a crumbled morphology of GNPs wrapped in hydration products, preventing crack propagation. The solid interfacial interaction between GNPs and the cement matrix facilitated effective stress transfer, enhancing the GNP-cement composite's flexural and compressive strength.

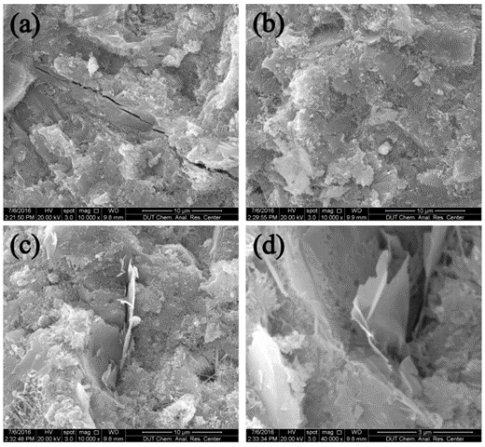

Figure 2.6 SEM images of (a) the plain cement paste and (b) the GNP–cement composite at the age of 28 days. (c) The GNPs inserted into the hydration productions of cement. (d) The plicate morphology of GNPs in cement. (Wang, Jiang, and Wu 2016)

(Du & Pang, 2015) investigated the transport and barrier properties of cement mortar with graphene nanoplatelet (GNP) concentrations of 0%, 2.5%, 5.0%, and 7.5% by weight of cement. While mechanical strength remained minimally affected, GNP inclusion significantly improved resistance to water permeability, chloride diffusion, and chloride migration by 30-70%. The optimal 2.5% GNP concentration showed over 30% reduction in critical pore diameter, providing 20% barrier effects against water and nearly complete

barrier effects against chloride ion ingress. Layered GNPs enhanced, which can be observed in Figure 2.7 pore structure and water pathway tortuosity, enhancing barrier properties, but concentrations above 7.5% resulted in nanoparticle aggregation and potential reduction in barrier efficiency.

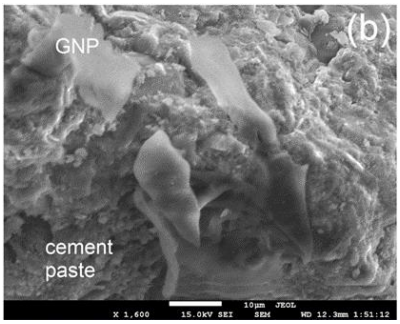

Figure 2.7 SEM images of GNP at the fractured mortar surface (Du and Pang 2015)

2.3.2 Carbon Nanotubes at Normal Temperature

(J. Huang et al., 2022) examined how multiwall carbon nanotube (MWCNT) concentration (0.05 to 0.70 wt.%). Specimens with dimensions of 40x40x160mm and a water-cement ratio of 0.4 were used. The optimal concentrations for maximum compressive and flexural strengths were determined to be 0.15% and 0.10% of MWCNT. The SEM micrographs in Figure 2.8 revealed that MWCNTs were thoroughly incorporated into the calcium silicate hydrate (C-S-H) structure, playing a bridging role that prevented crack initiation and growth, thus enhancing the mechanical properties of the composites. However, higher concentrations of MWCNTs led to agglomeration and the formation of micro-voids, which could reduce the mechanical characteristics of the composites. The study also observed that the mechanical strength increased slowly as hydration proceeded, influenced by different water-cement ratios.

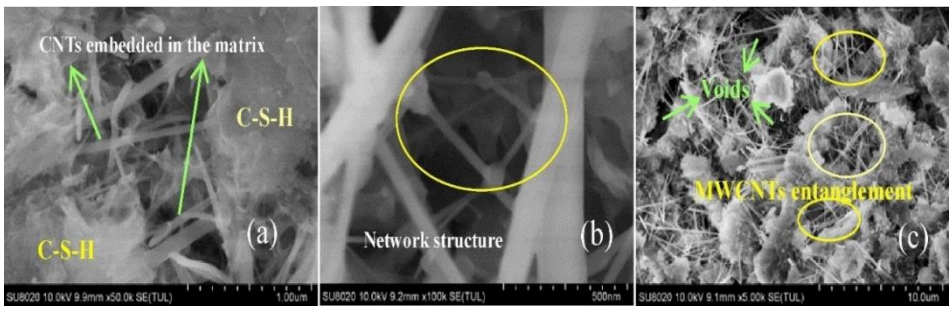

Figure 2.8 SEM images of MWCNT reinforced cement composites. a) MWCNT bridging action in the matrix b) microscopic network structure c) 0.3 wt% content of MWCNT. (Huang, Rodrigue, and Guo 2022)

(Muradyan et al., 2022) They have investigated the influence of Multi-Walled Carbon Nanotube (MWCNT) concentrations (0.001%, 0.01%, 0.05%, and 0.1% by weight) and sonication time (15 minutes and 40 minutes) on the compressive strengths of cement mortar. They were using a surfact`ant enhanced strength by improving MWCNT dispersion through decreased surface tension and better spreading and wetting characteristics. Optimal results were achieved with 40 minutes of sonication and a concentration of 0.01% MWCNTs, leading to uniform nanoparticle distribution and improved mechanical and physical properties of the cement-based mortars.

(Pinto, Dias, and Ribeiro 2022) They aimed to determine the optimal additive concentration for effective carbon nanotube (CNTs) dispersion and its impact on hydration and the physical-mechanical properties of cementitious matrices. Polycarboxylate-based superplasticizer proved most effective in CNT dispersion based on Zeta Potential analysis. Adding polycarboxylate-based CNTs to mortar exhibited a more significant increase in flexural strength (bridging effect) compared to compressive strength (filler mechanism). XRD studies revealed accelerated hydration with 0.075% and 0.100% CNTs, indicating their role as nucleating agents. CNTs displayed advantageous behavior in restraining nanoscale fractures, promoting stress transfer bridging and hydrated phase nucleation.

(Guan et al., 2020) investigated the influence of Multiwall Carbon Nanotubes (MWCNTs) on cementitious composites' mechanical characteristics and microstructures under freezing conditions at -15 °C. MWCNTs enhanced both the flexural and compressive strengths of cement pastes. Microstructural analysis revealed that MWCNTs acted as nucleating agents during hydration, reducing pore structure formation and binding cement's hydration products. SEM images supported crack bridging behaviour, enhancing the cementitious composites' mechanical properties. The study also discussed MWCNT behaviour in freezing environments.

(Konsta-Gdoutos et al., 2010) They have examined the integration of Multiwall Carbon Nanotubes (MWCNTs) in a cement paste matrix at various concentrations (0.025%, 0.048%, and 0.08% wt) with a w/c of 0.3 at room temperature. The study focused on nanomechanical properties, highlighting reduced porosity and enhanced high stiffness C-S-H (calcium-silicate-hydrate). Flexural strength tests revealed an optimum concentration

of 0.08% MWCNTs with small size (20-40 nm) exhibited favourable mechanical properties at 3, 7, and 28 days.

2.3.3 Graphene Oxide at Normal Temperature.

(Lu et al., 2022) demonstrated an efficient method of adding graphene oxide (GO) to cementitious composites to enhance the interfacial transition zone (ITZ) with sand particles. Mortar specimens with GO-pre-saturated sand at 0.05 wt% concentration by weight of cement showed a substantial increase in compressive (38%) and flexural strengths (44%) at 28 days. The mechanical improvement was attributed to thick polyhedral or flower-like hydration crystal formation by GO can be seen in Figure 2.9. Back-scattered electron imaging revealed a reduced ITZ thickness, leading to a denser microstructure and enhanced ITZ. The study emphasized the significance of nano-engineering ITZ with GO in cement composites for strength enhancement.

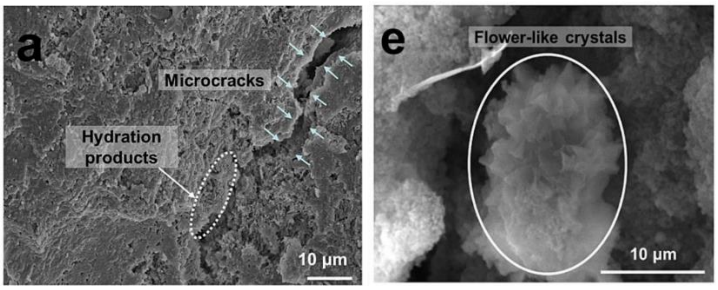

Figure 2.9 Typical SEM pictures of cement mortars GO@Sand (Lu, Shi, and Zhong 2022)

(S.-J. Lee et al., 2020) examined the impact of graphene oxide (GO) reinforcement on the workability and mechanical properties of cementitious composites at various replacement ratios (0, 0.01, 0.025, 0.03, and 0.05 wt% of cement's unit weight). Higher GO replacement ratios decreased workability due to water adsorption, reducing fluidity and increased friction between particles. From Figure 2.10 the optimal GO content was 0.025%, displaying the highest compressive strength of 48.1 MPa. GO's nano-2D structure influenced pore nucleation and filling, leading to a denser pore structure and enhanced particle load transfer. The study highlighted GO's role in influencing workability and mechanical properties in cementitious composites.

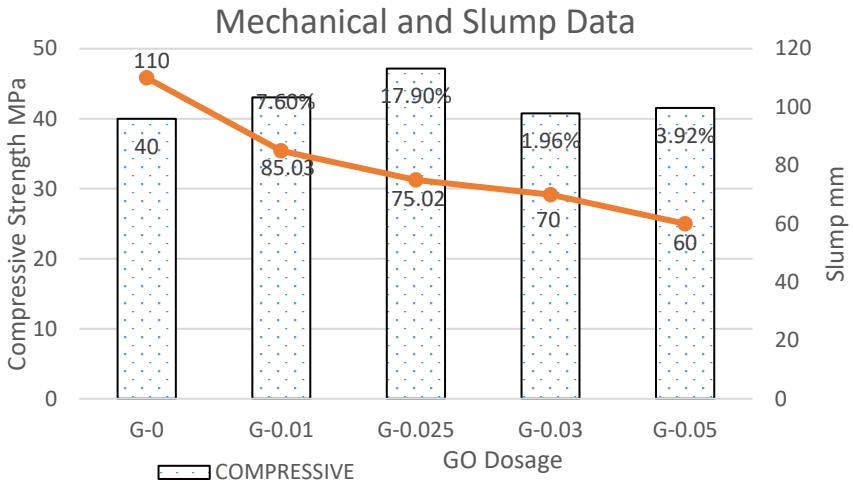

Figure 2.10 Mechanical and Workability property (Lee et al. 2020)

(Indukuri & Nerella, 2021) investigated the transport properties of graphene oxide (GO) in cement composites with different concentrations (0.01%, 0.02%, 0.03%, and 0.04% by wt of cement). Mechanical properties, thermal analysis, and chloride penetration depth were examined and compared to plain cement composites. Compressive and flexural strengths were highest at 0.04% and 0.03% GO, attributed to a more uniform distribution of hydration products and compact structure observed in SEM results. The addition of 0.03% GO decreased water absorption, sorptivity, and chloride penetration depth by 15-40%, signifying improved transport characteristics. However, GO concentrations above 0.04% led to nanoparticle aggregation and harmed transport properties.

(Naresh Kumar et al., 2021) conducted a comprehensive study on graphene-based nanomaterials, particularly graphene oxide-based nanomaterials, in cement and concrete composites at varying dosages (0.0%, 0.02%, 0.04%, 0.06%, and 0.08%). The incorporation of graphene oxide (GO) reduced the workability of cement-based materials due to its broad surface area, which could be mitigated with polycarboxylate ether-based superplasticizers. Moreover, GO inclusion enhanced the compressive strength of cement-based composites, attributed to its hydrophilic nature facilitating the hydration cycle. The study recommended further investigations into the durability properties of GO in cement composites.

(Zhao et al., 2020) conducted a comprehensive review on the reinforcing effects of graphene oxide (GO) on cement composites. The study emphasized the importance of

even GO dispersion within the cement matrix for effective nano-reinforcement, achieved through the successful strategy of using Polycarboxylate Ether (PCE) to stabilize the negative charge on GO sheets in the alkaline cement solution. Incorporating small amounts of GO improved the compressive strength of the cement composites, with TGA analysis confirming the hydrophilic nature of GO promoting early-age hydration and densifying pore structure. Furthermore, the addition of GO enhanced durability by improving resistance to carbonation and impeding the transit of aggressive agents within the cement matrix

(Peng et al., 2019) investigated the influence of graphene oxide (GO) content (0%, 0.01 wt%, 0.03 wt%, and 0.05 wt%) and water/cement (w/c) ratio on the mechanical properties and microstructure of GO-cement composites. The study found that the highest compressive strength was achieved at 0.01 wt% GO, while the highest flexural strength was observed at 0.03 wt% GO, indicating improved toughness of cement materials. SEM analysis revealed that higher w/c ratios facilitated better GO dispersion, leading to enhanced nucleation sites for hydration reactions in cement-based composites.

2.3.4 rGO (reduced graphene oxide) at Normal Temperature.

(Kong et al., 2022) investigated the impact of different reduction times and reducing agent (Vitamin C) dosages on the surface oxygen concentration of reduced graphene oxide (rGO). The study synthesized various rGO samples with different oxygen concentrations and added them at 0.1% dosage to cement-mortar composites. Results indicated that 50% Vitamin C reduction for 30 minutes proved highly effective in enhancing transport properties. Cement mortar with optimal oxygen concentration of rGO showed reduced carbonization depth and chloride ion penetration, with significant improvements in microstructure. Effective dispersion of rGO resulted in flower-like structures in Figure 2.11 and reduced contact between harmful substances and hydration products, improving overall properties of cement-based composites.

(Jayachandra et al., 2022) studied the mechanical behavior of cement mortar with varying concentrations of reduced Graphene Oxide (rGO) (0.02% to 0.1%). Compressive strength tests revealed maximum strength with 4-hour sonication at 3, 7, and 28 days. Incorporation of 0.1% rGO improved molecular bonding, hydration degree, and crystallinity during the curing process of the cement composite.

a

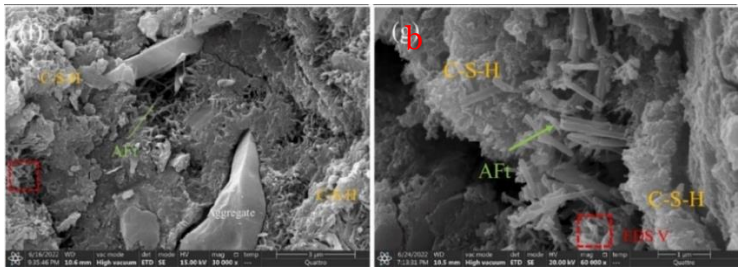

Figure 2.11 SEM pictures of the micromorphology of cement mortar at 28d (Kong et al. 2022).

(Zhai et al., 2021) investigated the effects of reduced Graphene Oxide (rGO) content represented in Table 2-2 (0 wt% to 4.00 wt%) and different dispersants on cement mortar properties. The water-Naphthalene superplasticizer (NS) - rGO suspension demonstrated ideal dispersibility and stability. The addition of 2.00 wt% rGO improved electrical resistivity, thermal conductivity, and electromagnetic shielding effectiveness of cement-based materials. Mechanical tests revealed an optimal rGO content of 2.00 wt%, which increased compressive and flexural strength at various curing times. However, at higher rGO concentrations (4.00 wt%), strength declined due to rGO aggregation. The study highlights the potential of rGO in enhancing cement properties for health monitoring devices.

Table 2-2 Properties of six different dispersants (Zhai et al. 2021)

Name of dispersants	**Name abbreviation**	**Water-reducing rate**
Naphthalene superplasticizer	NS	20%
Polycarboxylic superplasticizer	PC	40%
Aliphatic superplasticizer	SAF	20%
Sodium polystyrene sulfonate	PSS	-
Polyvinylpyrrolidone	PVP	-
Sodium dodecyl benzene sulfonate	SDBS	-

(Jing et al.2020) investigated the impact of oxygen-containing functional groups on reduced graphene oxide (rGO) in cement paste. GO levels of 0%, 0.3%, and 0.6% by weight of cement were examined. Mechanical tests revealed that 0.3% rGO with oxygen functional groups exhibited enhanced early-age compressive strength (8.19 MPa at 3

days) compared to 0.6% (2.91 MPa at 28 days). SEM images Figure 2.12 confirmed increased hydration products and denser microstructure in 0.6% rGO with oxygen group

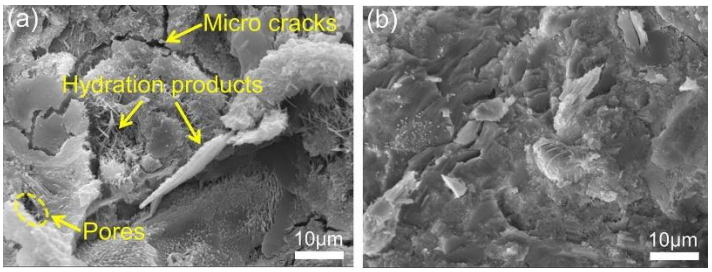

Figure 2.12 Micromorphology of hardened cement paste without annealing treatment (a,b) with annealing treatment (c,d) after 28 days curing (Jing et al. 2020)

(Valizadeh Kiamahalleh et al., 2020) investigated the impact of reduced graphene oxide (rGO) with different sonication times (1-8 h) and dosages (0.05-0.2%) on physicochemical and mechanical properties of cement mortar composites. Optimum results were achieved with 4h sonication time and 0.1% rGO content, showing increased hydration degree and reduced particle size. Good dispersion resulted in less agglomeration and enhanced CSH, as supported by SEM images Figure 2.13

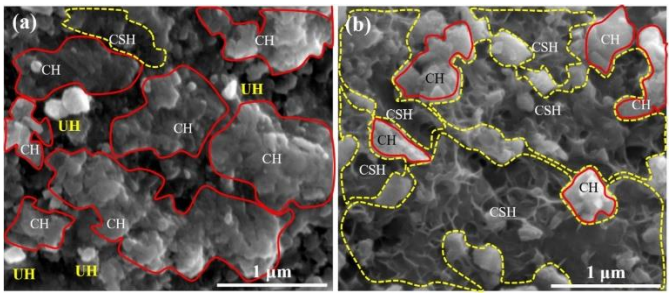

Figure 2.13 SEM images of surface structure of (a) plain cement mortar and (b) composite with optimum rGO (Valizadeh Kiamahalleh et al. 2020

(Qureshi & Panesar, 2020) investigated the influence of graphene-based 2D nanomaterials (GO, rGO, and G) on cement paste composites at concentrations ranging from 0.01% to 0.16% by weight. The optimal incorporation of 0.04% rGO at 28 days significantly improved cement hydration and mechanical properties, due to its low number of functional groups, physical strength, and water dispersibility. Compared to the control mix, the 28-day compressive and flexural strength of rGO cement composites increased by 30% and 84%, respectively, with minor impact on workability and reduced sorptivity by about 28%

(Qureshi & Panesar, 2019) compared the effects of GO and rGO at 0.02%, 0.04%, and 0.06% by weight of cement on workability, microstructure, mechanical, and transport properties. rGO showed better workability by increasing final setting time, while GO exhibited a loss of workability with increasing content due to its hydrophilic nature. Both GO and rGO at 0.04% content demonstrated optimal mechanical performance, enhancing cement hydration and forming strong covalent bonds with cement hydration products. SEM images Figure 2.14 showed that GO and rGO strengthened the microstructure by stimulating nucleation and bridging at the nano-micro level.

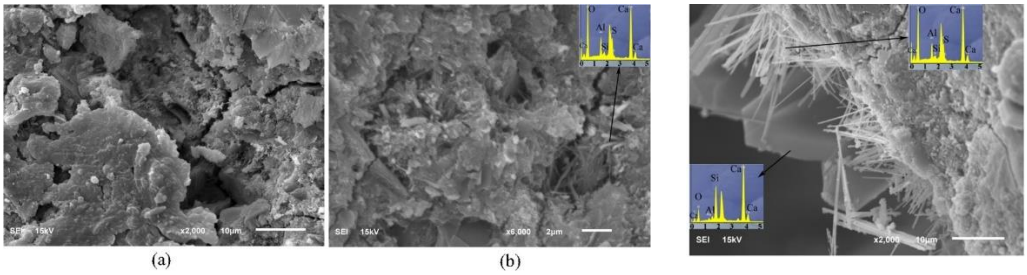

Figure 2.14 SEM images of surface: (a) REF. Sample (b) Microstructure characteristics in 0.06% rGO. (c) 0.06% GO (Qureshi and Panesar 2019)

(Gholampour et al., 2017) investigated the effect of graphene oxygen functional groups and structure defects on mechanical properties of graphene-cement mortar composites. Different rGO amounts (0.1%, 0.15%, 0.2%, 0.3%, and 0.4% by weight) were studied with various sonication times (5, 10, 15, 30, and 60 minutes) for better dispersibility. Results showed that using 0.1% rGO with 15 minutes reduction led to a substantial increase in 28-day tensile and compressive strengths (45.0% and 83.7%, respectively) compared to standard cement mortar composites. This enhancement was attributed to the highly hydrophilic and dispersible nature of 0.1% rGO with a dense spread of oxygen functionalities, impacting the physicochemical and mechanical properties.

2.3.5 Carbon Black at Normal temperature

(Zhang et al., 2022) investigated Carbon Black (CB) behavior in mortar specimens with varying contents (0%, 2%, 4%, 6%, and 8% by weight of cement). The addition of 2% CB resulted in a 26.6% increase in 3-day compressive strength and a 7.3% increase in 28-day compressive strength, attributed to improved cement material compactness due to the filler effect. However, flexural strength decreased by 56.3% at 3 days due to potential binder strength reduction in hydration products. Microstructural analysis in Figure 2.16

showed enhanced hydration products, optimized ITZ (Figure 2.17), reduced porosity, and increased density. SEM and BSE images supported the microscale refining effect, strengthening the hardened cement paste.

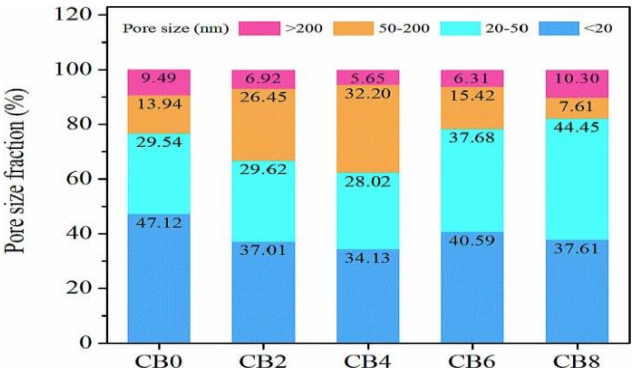

Figure 2.15 Pore size distribution among 28 d samples with varying CB contents. (Zhang et al. 2022)

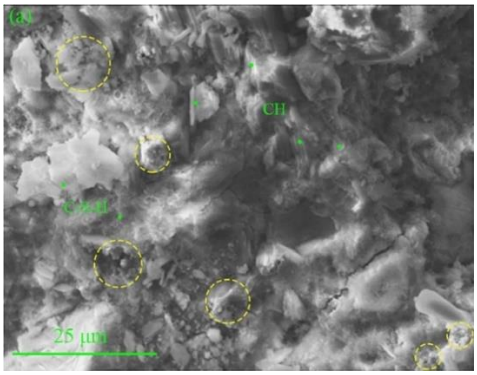

Figure 2.16 Microstructure analysis of cement paste with 2% CB. (Zhang et al. 2022)

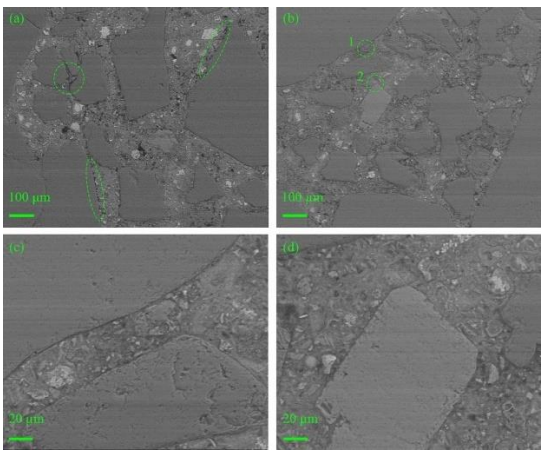

Figure 2.17 BSE images of ITZ in mortar samples: (a) without CB. (b) with 2% CB. (c), (d) the magnified images of position 1 and 2 in (b). (Zhang et al. 2022)

(Nalon et al., 2020) investigated the effects of various Carbon Black nanoparticles (CBN) at 8% weight of cement in smart mortars. Compressive strength results Figure 2.18 showed that higher CBN content decreased compressive strength due to poor cohesiveness between the cement matrix and CBN aggregates, hindering hydration. Blacks XC72, XC305, and XC605 with higher specific surface areas and structures had more significant strength reductions represented in Figure 2.18, attributed to increased water adsorption affecting cement hydration. N234 blacks, with lower structure and medium surface area, showed the least reduction in strength. Further research is needed to optimize water-to-cement ratio, CBN concentration, and type for desired electrical properties without major compressive strength loss.

Table 2-3 Different Type of CBN Properties

CBN type	Mix Name	Specific surface area (m^2/g)	Electrical resistivity (Ω.cm)
N234	CBN-125	120	3.3–3.9
Vulcan XC305	CBN-131	72	1.2–1.8
Vulcan XC605	CBN-148	90	1.7–2.1
Vulcan XC72	CBN-174	254	1.7–2.1

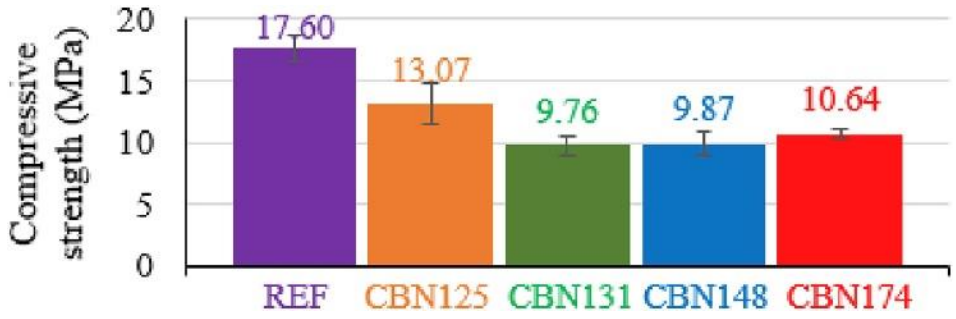

Figure 2.18 Mechanical strengthen properties of mortars with different types of CBN. (Nalon et al. 2020)

2.4 Mechanical Behaviour of Various Carbon-Based Nano-Cementitious Composites at Elevated temperature

2.4.1 Graphene Nanoplatelets at Elevated temperature

(Iqbal et al., 2020) investigated the effect of 2D Nano graphite filler (GNPs) concentrations (0.1%, 0.3%, 0.5% by weight of cement) on high strength concrete's mechanical properties at elevated temperatures200,400,600, and 800 °C. Compressive strength increased by 20%, 28%, and 24% with 0.1%, 0.3%, and 0.5% GNPs, respectively, due to filler action enhancing cement hydration. At 600°C, from Figure 2.19 compressive strength loss for 0.3% GNPs concrete was 57%, while for High Strength Concrete (HSC) it was 74%. GNPs' thermal conductivity distributed heat evenly and delayed fracture initiation and opening, preventing thermal degradation. Ultrasonic pulse velocity tests showed less damage and internal cracks in GNPs-modified samples after fire exposure. 0.3% GNPs was found optimal, enhancing interfacial bonding and serving as nucleation sites confirmed from SEM micrograph Figure 2.20. This study contributes to the understanding of GNPs' mechanism as nanofillers at elevated temperatures

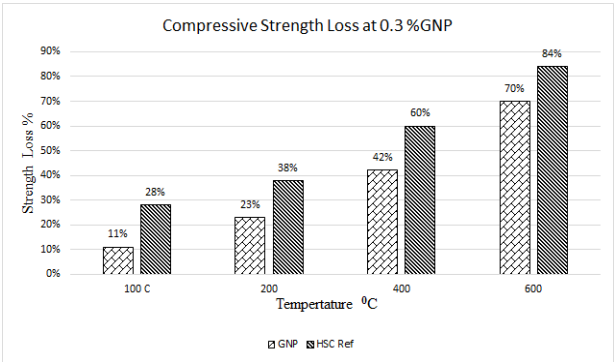

Figure 2.19 Normal temperature and High Temperature Comparison with respect to Strength loss. (Iqbal et al. 2020)

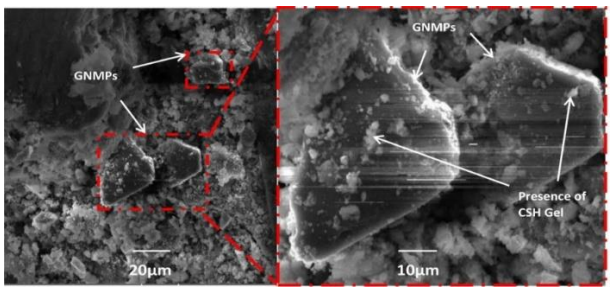

Figure 2.20 Micrograph of 0.3GNPs concrete after being exposed to elevated temperature of 400 °C (Iqbal et al. 2020).

2.4.2 Carbon Nano Tubes at Elevated Temperature.

(Sikora et al., 2019)) investigated the effect of Multi-Walled Carbon Nanotubes (MWCNT) concentrations (0.125 wt%, 0.25 wt%, and 0.5 wt%) and MWCNT with Nano silica (MWCNT/NS) on cement pastes with w/c 0.4. Heating specimens at 300, 450, and 600 °C revealed that 0.125%wt of MWCNT and MWCNT/NS improved microstructure and mechanical performance. After 28 days, no additional hydration strength was observed at 450°C, indicating low deterioration rate for MWCNT and MWCNT/NS. Figure 2.21 shows exceeding the optimal nanotube content led to agglomerations, reducing thermal resistance and resulting in lower strength values and micro cracking. These findings highlight the importance of optimizing MWCNT concentration for enhanced cement performance.

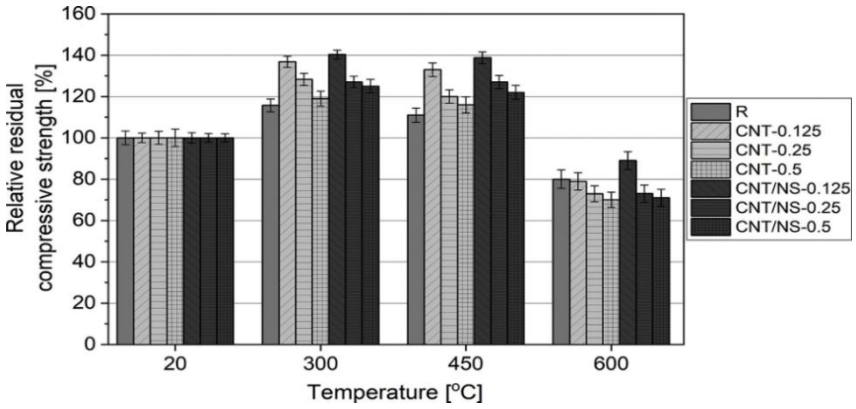

Figure 2.21 Mechanical Performance of MWCNT Concrete at High Temperature (Sikora et al. 2019)

(Sedaghatdoost & Behfarnia, 2018) In this investigation the impact of Multi-Walled Carbon Nanotubes (MWCNTs) on the strength of Portland cement mortar at high temperatures was studied. MWCNTs were added to the cement at concentrations of 0.05%, 0.1%, and 0.15% by weight. Mortar specimens of size 50 x 50 x 50 mm were prepared for residual mechanical performance. The specimens were subjected to heating at 200, 400, 600, and 800 °C at a heating rate of 20 °C/min in an electric furnace. Measurements were taken before and after heating, and the compressive strength results showed a decline in strength from 200 to 400 °C, with a more significant reduction observed between 600 and 800 °C.

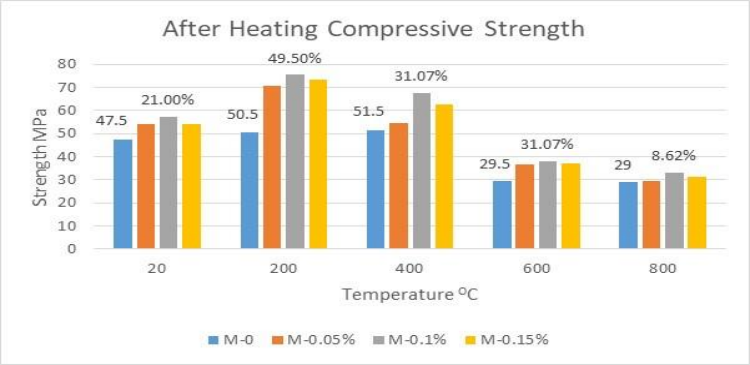

Figure 2.22 Compressive strength at different temperatures (Sedaghatdoost and Behfarnia 2018)

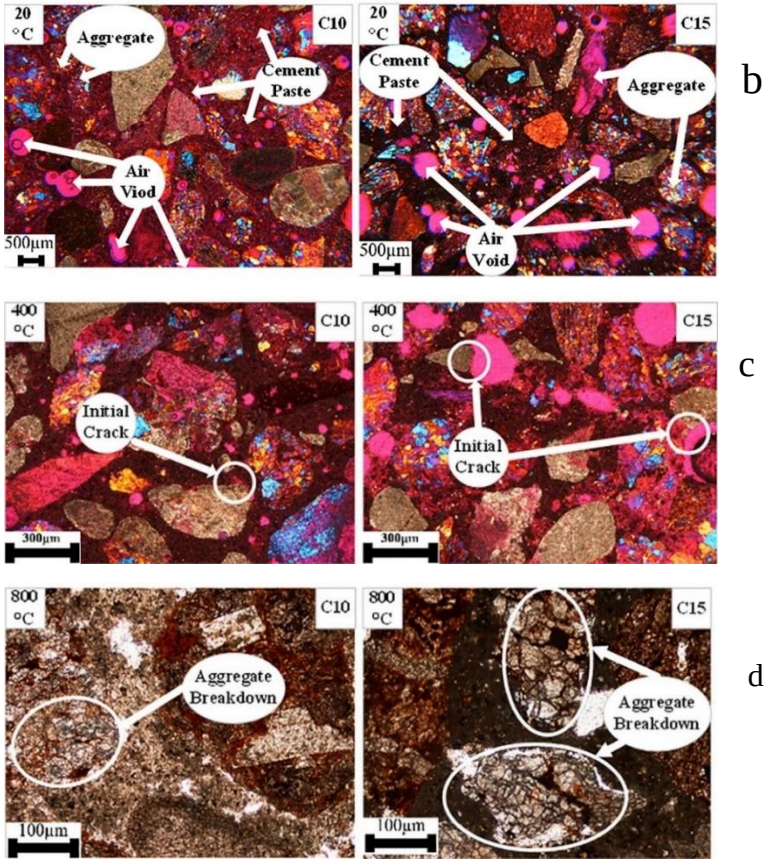

Figure 2.23 Petrography image at a) 20 °C. b) 400 °C c) 600 °C d) 800°C (Sedaghatdoost and Behfarnia 2018)

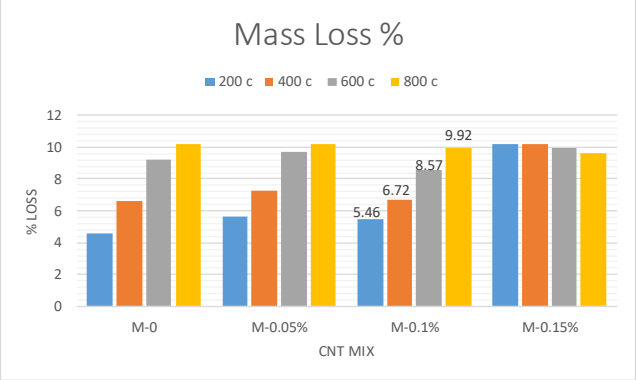

Figure 2.24 Results of the mass loss measurement (Sedaghatdoost and Behfarnia 2018).

However, the samples containing MWCNTs, especially at the 0.1% dosage, exhibited less strength decline and higher residual strength compared to the control sample .This enhancement was attributed to the denser microstructure of the MWCNT-containing specimens, which prevented water vapor escape. Petrography images Figure 2.23 revealed that MWCNTs contributed to a reduction in initial cracking at the Interfacial Transition Zone (ITZ). Samples containing MWCNTs at 0.1% weight percent of cement displayed higher compressive strength than other samples. Additionally, the thermal performance indicated that MWCNT-containing samples had lower mass loss Figure 2.24 during heating from 400 to 800 °C, further supporting the role of MWCNTs in maintaining the microstructure. The findings suggested an optimum MWCNT dosage of 0.1% for improved mechanical properties. However, the study highlighted the potential weakening of pink/red-discoloured cement paste and aggregate in the presence of MWCNTs. Overall, MWCNTs demonstrated the ability to enhance the residual compressive strength of mortar specimens at elevated temperatures, making them promising nanofillers for high-temperature applications in cement composites

(Baloch et al., 2018) investigated the impact of including 0.08% weight percent of Multi-Walled Carbon Nanotubes (MWCNTs) in both normal-weight and light-weight concrete. The concrete specimens were exposed to targeted temperatures of 200, 400, 600, and 800°C in an electric furnace, adopting a water-to-cement ratio of 0.5. Slow cooling in the furnace chamber for 24 hours was applied to avoid thermal shock during the residual test conditions. Mechanical performance revealed that MWCNT-modified concrete exhibited positive effects at normal temperatures compared to elevated temperatures, as shown in Table 2-4 Table 2-5. Microstructural analysis Figure 2.25 demonstrated the reinforcing

effect of MWCNTs, bridging the cracks and enhancing the strength of the samples. Additionally, light-weight concrete (LWC-MLWC) exhibited higher mass loss (14%) at 800°C than normal-weight concrete (NWC-MNWC) at 7%, attributed to the de-carbonation of calcium carbonate present in the limestone aggregate.

Table 2-4 Residual Compressive strength (Baloch et al. 2018)

Modified Concrete	TEMP °C	Strength loss
MLWC	400,600,800	28, 34, 66%,
MNWC	400,600,800	16, 33, 76 %
Normal Concrete		
LWC	400,600,800	23, 37, and 62%
NWC	400,600,800	18 ,49, 76%

Table 2-5 Residual tensile strength (Baloch et al. 2018)

Modified Concrete	TEMP °C	Strength loss %
MLWC	400, 600, 800	28,50, 88
MNWC	400, 600, 800	55, 70, 85
Normal Concrete		
LWC	400, 600, 800	26, 58, 92
NWC	400, 600, 800	60, 83, 85

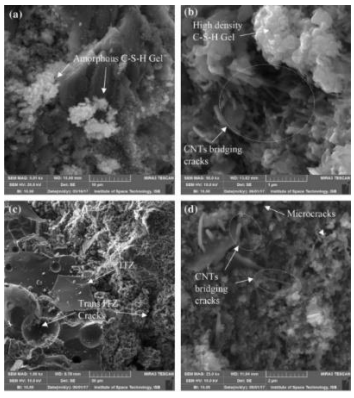

Figure 2.25 Micrographs concrete of samples exposed to 600°C: (a) Normal weight concrete. (b) Modified normal weight concrete. (c) Lightweight concrete. (d) Modified lightweight concrete (Baloch et al. 2018)

2.4.3 Graphene Oxide at Elevated Temperature.

(Han et al., 2022) conducted a study to explore the influence of graphene oxide (GO) on cement composites. The researchers found that the inclusion of 0.1 wt% GO yielded the highest compressive strength after 28 days. When subjected to elevated temperatures, the presence of 0.1 wt% GO facilitated the rapid densification of the microstructure, resulting in a less permeable matrix. However, excessive amounts of GO led to the formation of clusters, which increased the porosity of the cement and consequently diminished its strength. These findings underscore the significance of carefully selecting the appropriate concentration of GO to optimize the performance and properties of cement composites.

(Chen et al., 2022) investigated the high-temperature properties of cement pastes containing graphene oxide (GO) agglomerates at various temperatures (105°C, 200°C, 300°C, and 450°C). Two GO concentrations (0.02% and 0.04% by weight of cement) were examined. The study revealed that GO helped retain finer pore structures in sample CG4 after exposure to 300°C, preventing coarsening of the cement paste. Residual compressive strength Figure 2.28 exhibited non-linear losses due to high-temperature exposure, with increased strength observed at 200°C and 300°C, attributed to additional hydration. From Figure 2.26 the presence of GO promoted more non-evaporable water and enhanced hydration, beneficial for internal autoclaving conditions. The results concerning thermal and mechanical properties indicate that the incorporation of GO led to an increase in non-evaporable water content. This effect contributes to delaying the occurrence of microcracks or spalling over concrete when exposed to high temperatures

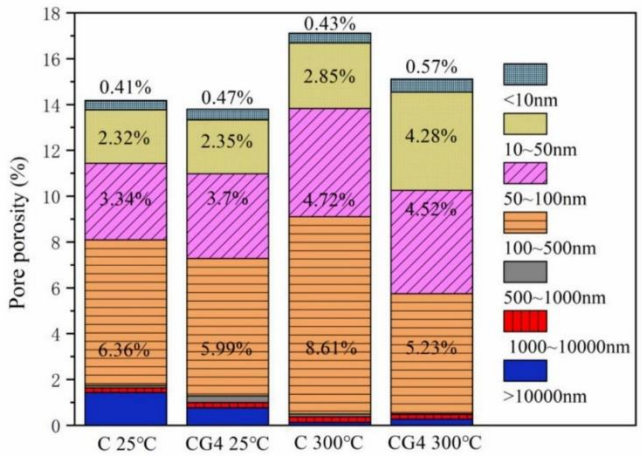

Figure 2.26 MIP Data at different temperatures. (Chen et al. 2022)

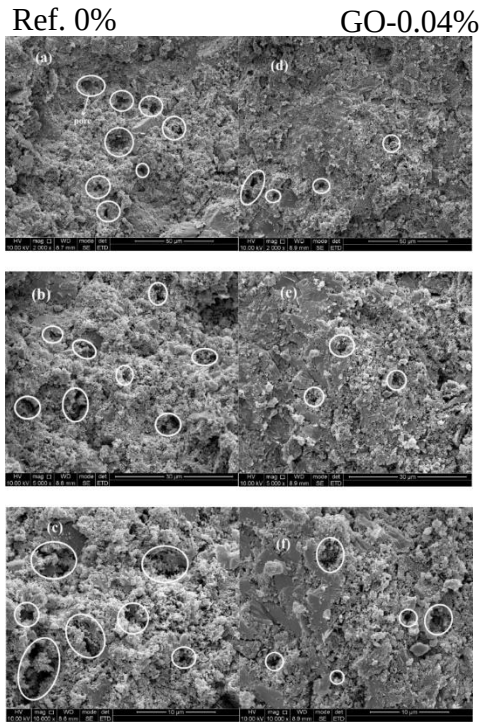

Figure 2.27 SEM analysis of GO with 0% and 0.04% (Chen et al. 2022)

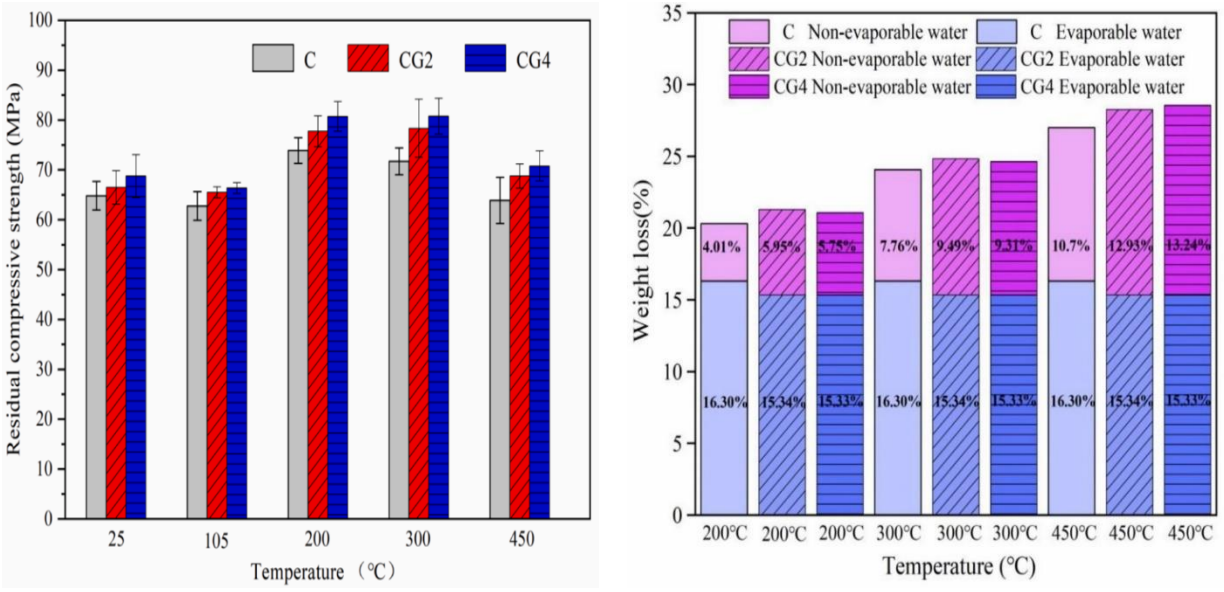

a) **b)**

Figure 2.28 a) Residual Mechanical Properties b) Non-Evaporable and Evaporable water content (Chen et al. 2022)

2.4.4 Reduced Oxide at Elevated Temperature.

(Prabavathy et al., 2020) studied the effects of rGO as an additive to cement mortar cubes at various percentages (0.05%, 0.1%, 0.15%, and 0.2% in w/c 0.5). Compressive strength testing revealed that 0.1% rGO displayed a higher strength of 24.02 MPa (63% increase) after 7 days and 36.23 MPa (44% increase) after 28 days compared to the control. SEM images Figure 2.30 showed needle-shaped structures aiding in hydration product development. After heating at 250 °C, residual strength demonstrated in Figure 2.29 0.1% rGO with 8.71 MPa strength, over 93% of the control. rGO-modified cubes exhibited positive stability against acid attacks due to their sheet-like morphology and void-filling ability. Carbonation depth at 0.1% GO was about 1mm, while control cubes had 2 mm (28 days) and 3 mm (56 days) depth.

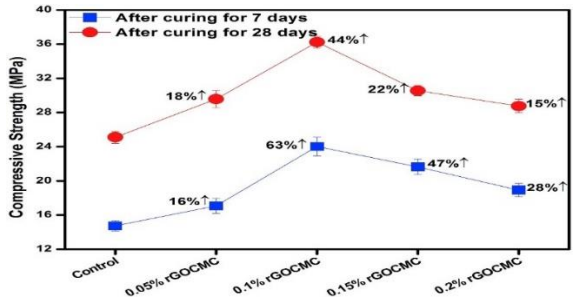

Figure 2.29 Compressive strength values of prepared specimens. (Prabavathy et al. 2020)

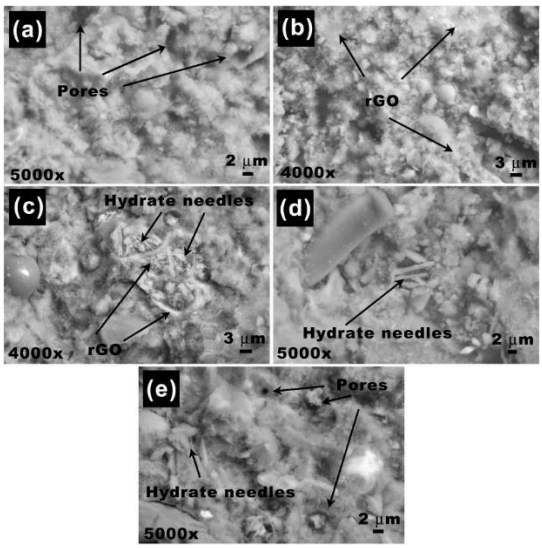

Figure 2.30 SEM images of crushed (a) Control mortar cubes, (b) 0.05% rGO, (c) 0.1% rGO, (d) 0.15% rGO, (e) 0.2% rGO. (Prabavathy et al. 2020)

2.4.5 Carbon Black at Elevated Temperature

(H. Lee et al., 2022) investigated the heating performance of carbon-based nanomaterials, including multiwalled carbon nanotubes (MWCNTs), conductive carbon black (CB), and graphene nanoplatelets (GNPs). The study evaluated different concentrations (0.25%, 0.50%, and 1.00% cement) and curing days on specimens' sizes of 50x50x50mm. Results indicated that 0.1% was the optimal content for carbon nanomaterials, with MWCNTs exhibiting the highest heating performance, followed by CB and GNP. Electrical resistance was lower in MWCNT cementitious composites compared to CB and GNP composites. From Figure 2.31 SEM images revealed the microstructure differences, supporting the exceptional heating and electrical performances of the MWCNT cementitious composite due to its homogeneous distribution.

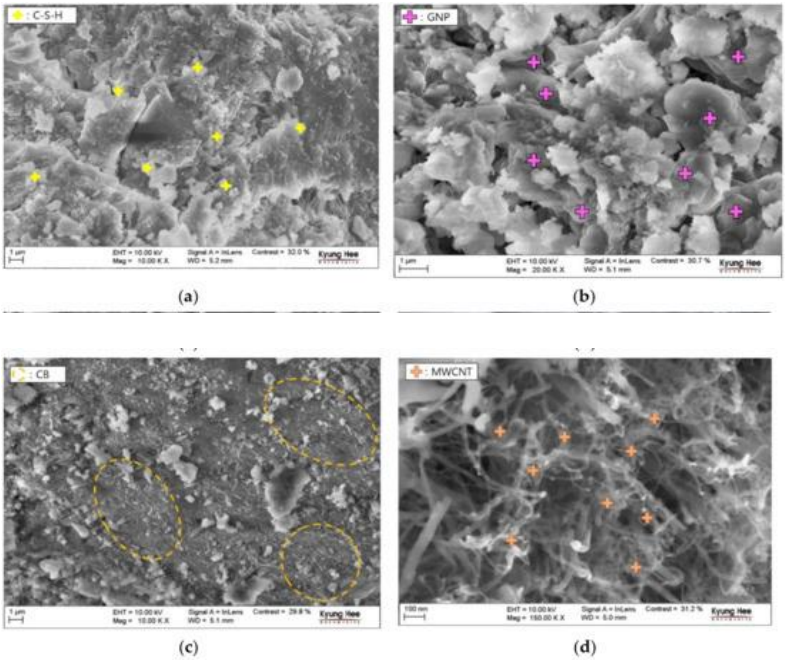

Figure 2.31 Field-emission scanning electron microscopy images: (a) OPC; (b) GNP-1.0; (c) CB-1.0; (d) MW-1.0. (Lee et al. 2022)

(Nalon, Ribeiro, de Araújo, et al., 2021) conducted an experimental investigation on mortars containing CBN (3%, 6%, 9%) and MWCNT (0.4%, 0.8%, 0.12%) by weight of cement exposed to high temperatures up to 600°C. Optimal performance in residual compressive strength was observed with 3% carbon black and 0.4% MWCNT. Nanomodified composites displayed higher residual strength than plain mortars after exposure to 600°C, attributed to the nanofillers' decomposition process releasing high-

pressure steam and improving pore system densification and chemical stability. However, composites with high CBN and MWCNT concentrations showed significant strength losses due to reduced C-S-H levels and poor cohesion. From Figure 2.32 SEM results supported these findings, showing improved bonding and stability at lower carbon black concentrations**.**

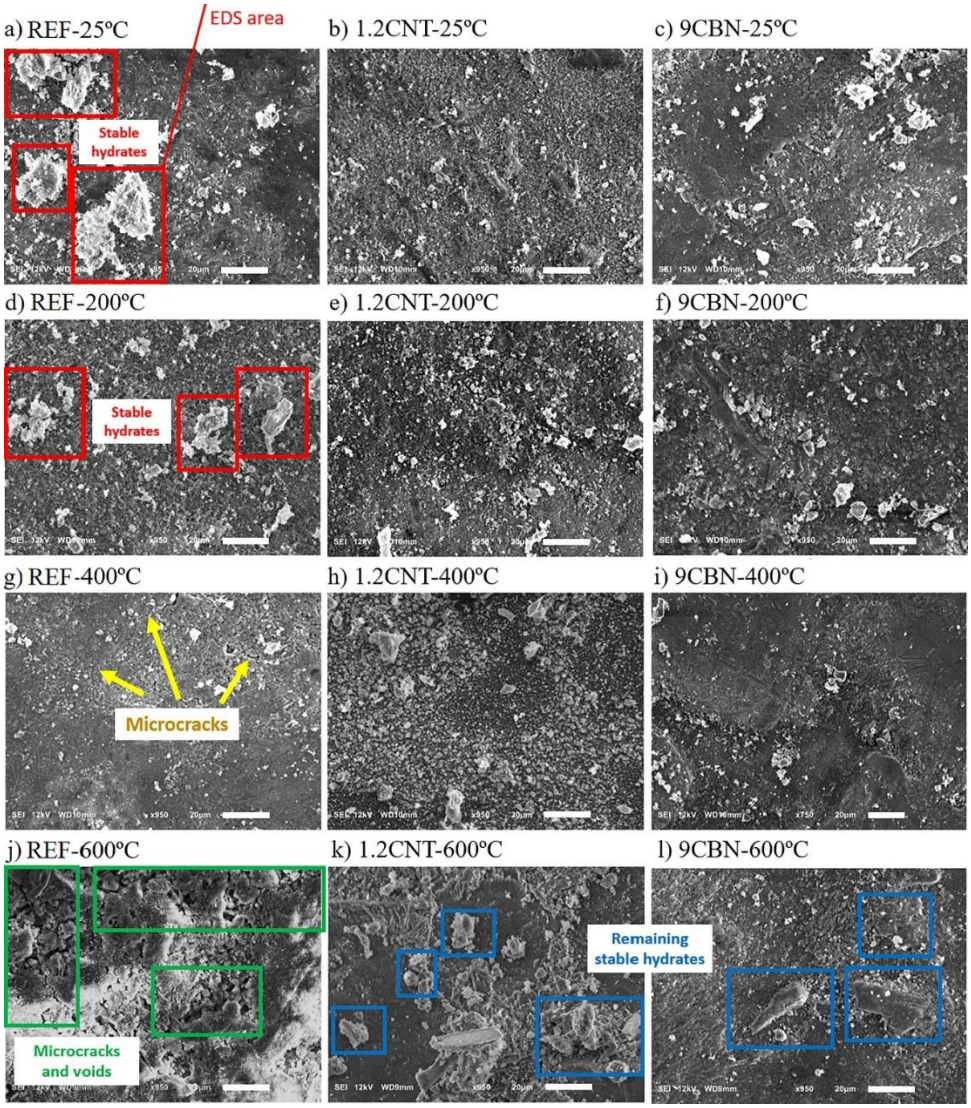

Figure 2.32 SEM results of plain and nanomodified cementitious matrices exposed to different temperature levels (Nalon, Ribeiro, de Araújo, et al. 2021).

(Nalon, Ribeiro, Araújo, et al., 2021) investigated the effect of post-fire curing on mortars containing different concentrations of MWCNT (0.4%, 0.8%, 1.2%) and CBN (3%, 6%, 9%) as nano reinforcements. Rehydration of specimens after fire exposure showed improved mechanical performance up to 400°C with nanofillers compared to normal

mortar. The nanomaterials provided extra nucleation sites for dehydration products to settle and rehydrate, enhancing post-fire curing at temperatures up to 400°C. SEM images Figure 2.31 supported the presence of hydrates produced by carbon nanomaterials. However, at 600°C, no improvement was observed as nanofillers began to decompose around 500°C, hindering rehydration reactions. Optimal concentrations were found at 0.4% and 0.8% for MWCNT and CBN, respectively, above which water access to decomposed C-S-H gel was inhibited.

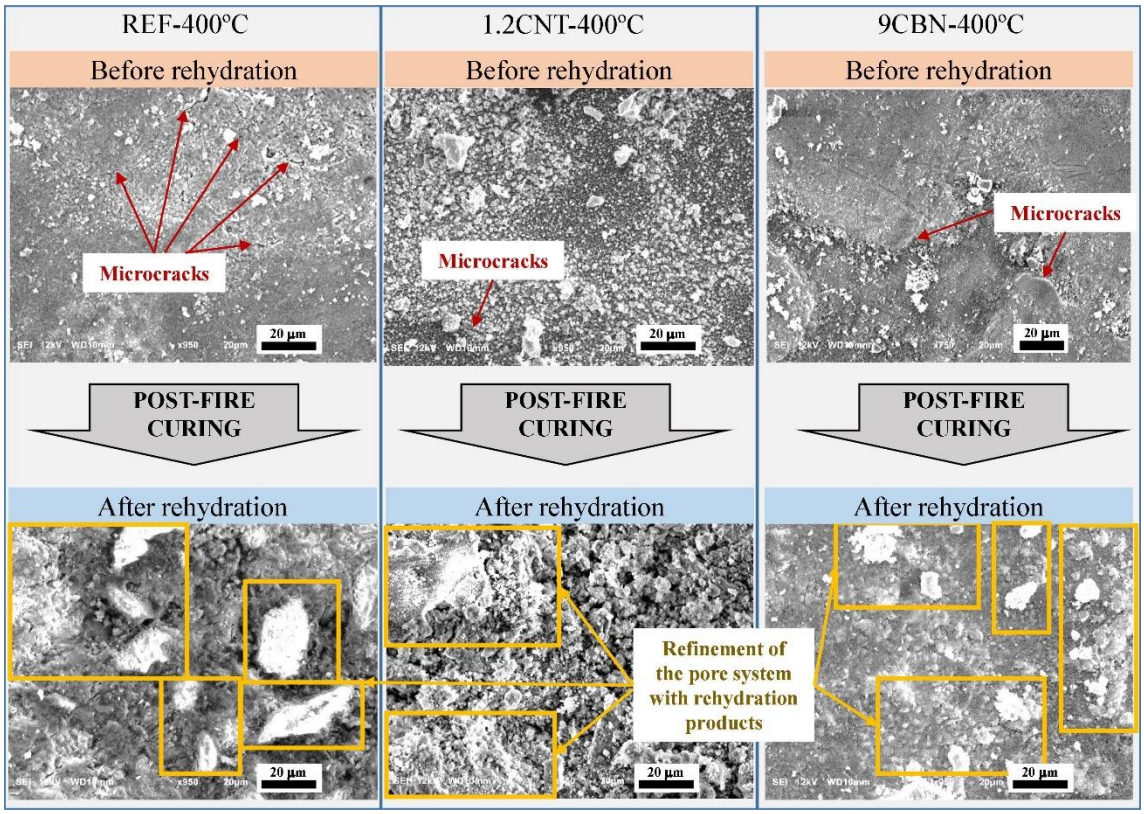

Figure 2.33 SEM of plain and nanomodified cement matrices exposed to 400 °C, before and after rehydration (Nalon, Ribeiro, Araújo, et al. 2021).

2.5 Research Gaps

The influence of nanocarbon black on the thermal resistance of cement pastes under high-temperature conditions remains relatively unexplored in the existing literature. While numerous studies have explored the mechanical and piezoresistive properties of cement-based materials containing nanocarbon black at room temperature, there is a notable absence of research that delves explicitly into the experimental analysis of the residual mechanical properties of cement-based materials with carbon black subjected to elevated temperatures of up to 800 °C. Furthermore, the cost-effectiveness of nanocarbon black

compared to other nanomaterials presents an unexplored avenue in cementitious composites. Its lower cost makes it an attractive candidate for potential industrial applications, but the extent of its influence on thermal resistance under high-temperature conditions remains unknown. Additionally, nanocarbon black, a waste product from the rubber tire industry, raises questions about its utilization for sustainable and environmentally friendly practices in cement composites. Despite its potential as a beneficial waste-to-resource material, the lack of in-depth research on its thermal performance at elevated temperatures hampers its full-scale adoption in cementitious applications.

Addressing these research gaps would expand the understanding of nanocarbon black's role in enhancing the thermal resistance of cement pastes and offer valuable insights into its economic viability and environmental impact. Filling this gap could lead to the developing of cost-effective, sustainable, and thermally resilient cementitious materials for various engineering applications in high-temperature environments.

2.6 Objective of Study

The inclusion of carbon black nanoparticles (CBN) in cementitious composites has garnered significant attention in the literature, primarily due to the good results obtained in terms of mechanical properties. The high surface area-to-volume ratio of Carbon black allows for enhanced reactivity and can fill the pores and microcracks within the cement matrix, resulting in enhanced densification hydration processes when incorporated into cementitious systems. This leads to improved strength development and densification of the composite matrix. Thus, based on research gaps and presented literature review following objectives are set for the present study :-

- To investigate the mechanical properties of nanoparticle modified cement-mortar at various replacement levels of cement.
- To check the thermal performance of developed cement mortar at different temperature regimes.
- To verify the results obtained during mechanical testing by using micro-structural analysis.

2.7 Significance of the study

This research focuses on comprehensively investigating the effects of increased temperature on vital properties of nano-engineered composite mortar, specifically compressive strength, flexural strength, and mass loss. The research methodology adopts a systematic approach, commencing with the determination of an optimal mix design through the implementation of trial mixes. Subsequently, mortar specimens are meticulously cast and subjected to rigorous testing, with thorough data analysis carried out. Advanced techniques such as X-ray diffraction and scanning electron microscopy are employed to observe and analyze the microstructural changes. The study aims to provide insights into how the inclusion of Carbon black influences the microstructure and mechanical characteristics of cementitious composites under high temperature conditions, contributing to a deeper understanding of the material's behavior in demanding environments.

Chapter 3

Experimental Programme

3.1 General

A comprehensive experimental program was designed to investigate the impact of carbon black nanoparticles (CBN) on various engineering properties of cement mortar. The experimental program consisted of three main elements:

- modification or compatibility of nano carbon black with cement mortar,
- fabrication and curing of cement mortar samples,
- evaluation of the mechanical properties of the cured cement mortar at elevated temperatures, and

Microstructure analysis of the characteristics of the hardened cement mortar. This chapter presents a comprehensive description of the phases of the experimental program conducted as part of the research project, including the outcomes obtained from each phase.

3.2 Methodology schematic representation.

A schematic representation of methodology, referred to as a research methodology diagram or flowchart, is a visual depiction of the systematic approach researchers follow to conduct a study or investigation. This representation serves as a roadmap for both the researchers themselves and their audience, providing a clear and concise overview of the steps, processes, and methods employed in the research project. It helps in conveying the research plan, making it easier to understand and evaluate. Figure 3.1 give the schematic representation of our study.

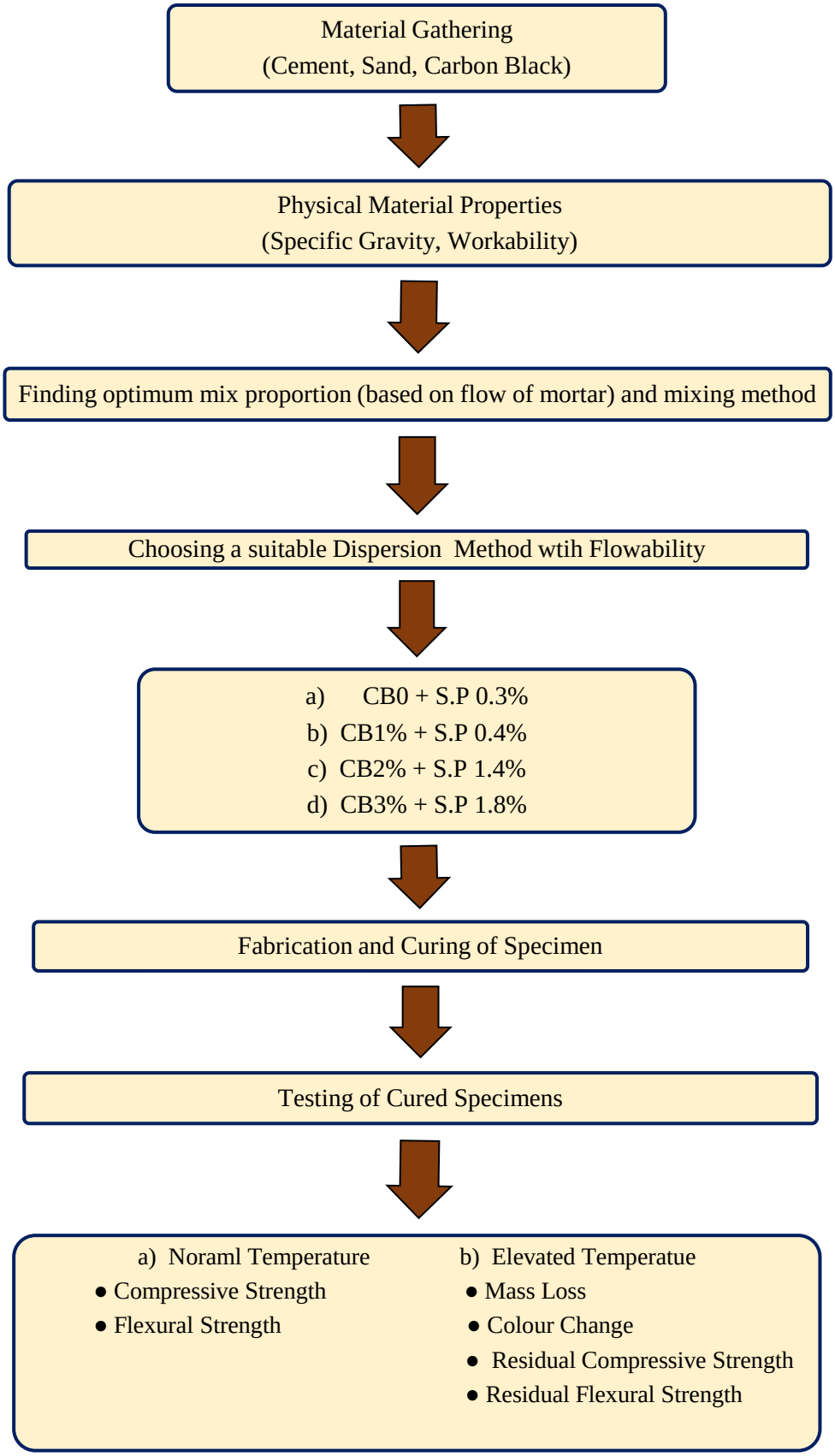

Figure 3.1 Schematic Representation of study

3.3 Raw Materials Employed in the Present Research

This section thoroughly examines the materials employed in the experimental work to produce polymer-modified mortar mixes. Laboratory analysis, conducted following the appropriate IS codes of practice, aimed to evaluate these materials' chemical and physical properties. The primary constituents used in the study encompass cement, fine aggregates, water, and carbon black nanoparticles, blended in different ratios. Subsequent subsections comprehensively depict each material, including a detailed exploration of their properties, granting valuable insights into their function and attributes within the current experimental investigation.

3.3.1 Ordinary Portland Cement

The production of Ordinary Portland cement, 43 grade, involves thoroughly blending calcareous and argillaceous materials and other silica, alumina, or iron oxide-bearing substances. These components are subjected to a clinkering process at an appropriate temperature, followed by grinding the resulting clinker to produce cement that meets the specifications outlined in the relevant standard. Cement serves as the highly reactive element in mortar. The careful choice and appropriate utilization of cement play a crucial role in achieving the optimal cost-effective combination of desired properties for a specific mixture. Cement functions as a pozzolanic material, demonstrating the capability to form a dense matrix when combined with aggregates, thereby contributing to structural strength. Its primary role involves filling the voids between fine aggregates, leading to the creation of impermeable concrete. Cement undergoes a hydration reaction upon adding water, forming CSH (calcium silicate hydrate) gel. This gel acts as a link between particles, enabling their binding and cohesive properties. Cement establishes a robust bond among the aggregates by setting and hardening in the presence of water, forming a solid mass and substantially enhancing the concrete's overall strength. Ordinary Portland Cement (OPC) has been utilized in this research. The cement was sourced from nearby suppliers (Shree Cement). Figure 3.2 shows the texture of OPC-43 presents, and Table 3-1 physical properties of cement determined through multiple experiments conducted by the Indian Standard (IS; 8112 2013). The properties evaluated include the initial and final setting time, specific gravity, fineness, and compressive strength, among other essential tests for cement characterization.

Figure 3.2 OPC-43

Table 3-1 Physical Properties of Cement used in the study

Characteristics	Value	Code to be followed IS- 8112:2013
Grade	OPC-43	OPC- 43
Specific Gravity	3.12	3.10-3.25
Standard Consistency (%)	28%	28 %
Initial Setting time	110 min	30 min (Minimum)
Final Setting Time	262 min	600 min (Maximum)

3.3.2 Fine Aggregates

According to (IS, 383 1970) fine aggregate is categorized into four grading zones (Grades I to IV), determined based on the particle size distribution. The grading zones progress from coarser in Zone I to finer in Zone IV. To prepare the fine aggregates for use, they underwent a thorough washing process to eliminate any silt and clay present. Subsequently, the aggregates were subjected to 24 hours of oven drying. After reaching room temperature, they were incorporated into the mixture.

The present study incorporates natural river sand classified as Zone II. Table 3-3 presents the sieve analysis results, offering insights into the particle size distribution. Based on IS 383 (Table 4), the fine aggregates used in the study were categorized as ZONE II. An experimental procedure specified in IS 2386-part III (1963) was employed to determine their specific gravity, utilizing the pycnometer. The specific properties of the sand, such as its specific gravity and water absorption, are given in Table 3-2 were examined. This

summary highlights the classification of the aggregates, the experimental approach taken, and the obtained specific gravity measurement.

Figure 3.3 Physical Representation of Sand

Table 3-2 Physical Properties of Sand

Physical Properties	**IS Specifications 2386-1963**
Specific Gravity	2.64
Water Absorption	0.30%
Colour	Greyish

Table 3-3 Sieve Analysis of Fine Aggregates

S.No	**IS Sieve (mm)**	**Wt. Retained (gm)**	**Percentage Retained**	**Percentage Passing**	**Cumulative Percentage Retained**
1	4.75	24	2.4	97.6	2.4
2	2.36	86	8.6	89	11
3	1.18	191	19.1	69.9	30.1
4	600	151	15.1	54.8	45.2
5	300	259	25.9	28.9	71.1
6	150	247	24.7	4.2	95.8
7	Pan	42	4.2	-	-
TOTAL		1000		SUM	255.6
ZONE II		F.M = 2.56			

3.3.3 Water

This study used ordinary tap water to mix and cure cement mortar, which complied with IS: 456-200 standards. The water, with a pH greater than 6, played a crucial role in the chemical reaction with cement. It facilitated the formation of cement gel, contributing to the strength of the mortar. Careful consideration of the water's quantity and characteristics is essential for optimal results.

3.3.4 Admixtures

A superplasticizer is crucial in nano cementitious to improve workability and prevent agglomerates' formation. The nanoscale particles provide a larger surface area, leading to agglomerates forming. The formation of agglomerates in a cement matrix causes an area of high-stress concentration, leading to the initiation of cracks and a reduction in strength. This issue can be addressed by employing suitable surfactants to prevent agglomeration (Monteiro et al., 2015).

In this study, a polycarboxylic ether-based superplasticizer (SP), as shown in Figure 3.4 was utilized, meeting the specifications of (IS, 9103:1999) , ASTMC-494 type F, and. It had an approximate density of 1.10 and a pH value of around 5.0. The superplasticizer dosage was adjusted to attain a consistency similar to their control mixes, per the guidelines outlined in (ASTM, 1437-2007)

Figure 3.4 Colour Property of SP

Table 3-4 Properties of Poly carboxylate ether (PCE) superplasticizer

Property	Value
Colour	Light Brown Liquid
pH	≥6

3.3.5 Carbon black

Carbon black is a fine particle Figure 3.5 composed of elemental carbon, primarily produced by incomplete combustion or thermal decomposition of hydrocarbons. It comprises tiny particles with a large surface area and possesses high conductivity, exceptional UV resistance, and potent pigmenting abilities. Carbon black finds various applications across different industries. In the rubber industry, it is extensively used as a reinforcing filler in tires and other rubber products to enhance their strength, durability, and wear resistance. It is also utilized as a pigment in inks, coatings, and plastics due to its ability to provide deep black colour.

(Donnet et al., 2018) Use of nanocarbon black as nanoengineered Cementitious material enhanced performance and beneficial microstructural change in the cement paste (J. Zhang et al., 2023). Carbon Black Nanoparticles (CBN) are generally found to be less than 300 nm in size (Bera et al., 2019) Including CBN in the cement compositions offer several advantages similar to those of various expensive conductive additives but at a significantly lower cost. This is due to the remarkable characteristics of CBN, including its large surface area, small particle size, excellent electrical conductivity, and affordable production process (Y. Huang et al., 2018)

The SEM image in Figure 3.6(a) demonstrates that CBN has a bud-like structure. In Figure 3.6(b), X-ray diffraction (XRD) analysis revealed the amorphous nature of Carbon Black (CB), as specific peak patterns could not be identified. However, the presence of broader and more intense peaks at 2θ angles around 20 and 30 degrees suggests some degree of structural order within the material similar pattern observed in the (Irshidat et al., 2021) Despite the lack of distinct crystalline patterns, these findings indicate potential interactions and arrangements within amorphous CB.

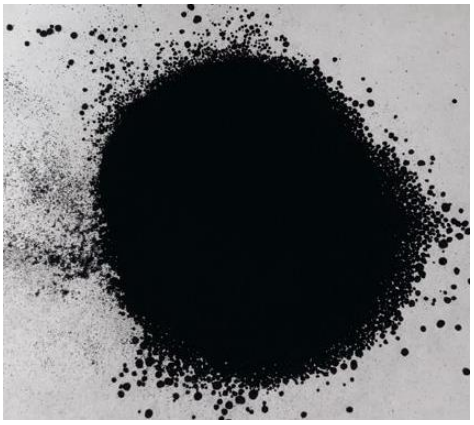

Figure 3.5 Carbon Black

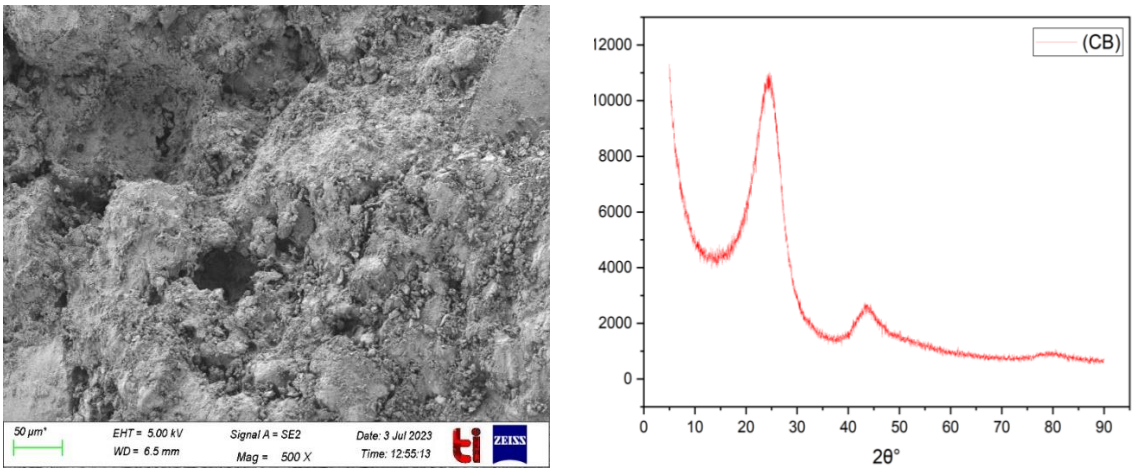

a) **b)**

Figure 3.6 a) SEM image b) XRD Pattern

3.4 Preparation and fabrication of specimens.

3.4.1 Mix Proportion

The mix proportioning employed in the present investigation was designed in conformity with (ASTM,C 109,2005) and shown in Table 3-5. CB content was varied from 0 to 3% by weight of cement in the mix In.CB1 CB shows the replacement of Carbon black and numeric number 1 shows the replacement of cement by 1%. CB0 deminstrates the control specimen or specimen without any replacement. Mortar samples were made with a binder-to-sand ratio of 1:2.74 and a water-to-binder ratio of 0.48 in order to assess the effects of carbon black nano powder additions on compressive strengths. Adequate mortar

flow was achieved by using different levels of a superplasticizer as a water-reducing agent. (Monteiro et al., 2015)

Table 3-5 Concentration of Different Mix Proportions

Blends	Designation ID	SAND/BINDER	WATER/BINDER	SP %	CB %
OPC	CB0	2.75	0.48	0.3	0
OPC+1%CB	CB1	2.75	0.48	0.4	1
OPC+2%CB	CB2	2.75	0.48	1.4	2
OPC+3%CB	CB3	2.75	0.48	1.8	3

3.4.2 Fabrication Of Mortar Samples

In order to examine the properties of mortar, a mixture of cement and sand was used in a ratio of 1:2.75 with w/c 0.48. The tables, namely Table 3-6 and Table 3-7, illustrate the specimens employed for investigating the cement mortar's mechanical properties and microstructural analysis. These tables provide a comprehensive overview of the specific specimens used in each analysis, allowing for a systematic examination of the various aspects of the cement mortar's mechanical behaviour and microscopic characteristics.

3.4.2.1 Procedure Followed

In accordance with ASTMC-109, the casting of specimens was carried out following a given specific procedure in the code. Initially, all the materials required for the mix were weighed according to the predetermined proportions. Subsequently, the weighed materials and the necessary amount of water were added to the dry bowl of a digital mixer. After that, the mixer ran for 60 seconds. After 60 seconds, the mixer was turned off for 15 seconds so that any paste stuck to the edges of the bowl could be scraped into the mixture. Then, after restarting the mixer at a medium speed of around 285 10 revolutions per minute, another minute of mixing was completed.

The material was carefully poured into oiled moulds after it reached the correct consistency, filling each form to the top. Then, each compartment of the cube moulds was filled with a layer of mortar measuring roughly 25 mm thick. The mortar in each compartment was compacted by tamping it 32 times within a time frame of around 10 seconds, conducted in four rounds. The moulds were vibrated in order to release any

trapped air. By dragging a trowel's straight edge over the top of the mould, the extra mortar was scraped off to create a flat surface.

Immediately after the completion of the moulding process, the test specimens were transferred to a moist room and left undisturbed for 24 hours. This step aimed to provide the specimens with an optimal curing environment to enhance their strength development and facilitate subsequent microstructural analysis.

Table 3-6 Specimen Specifications for Mechanical Properties

Test	Specimen Type	Dimensions
Compression	Mortar Cubes	50x50x50 mm
Flexural	Mortar Beams	40x40x160 mm

Table 3-7 Specimens Employed for Microstructural Analysis

Specimen	Test
Mortar chunks	Scanning Electron Microscopy (SEM)
Mortar Powder	X-Ray Diffraction

3.5 Experimental programme

3.5.1 Different Type of Dispersion Methods

Nanotechnology encompasses a broad range of disciplines that deal with materials, structures, or objects at a microscopic scale. Nanomaterials are typically characterized by their lengths, which can range from sub-nanometres to several hundred nanometres. The incorporation of nanoparticles into cementitious materials has demonstrated significant improvements. This is mainly attributed to the large surface area of nanoparticles, which enhances their chemical reactivity. The increased surface area facilitates the formation of hydration products by providing numerous nucleation sites. Consequently, this phenomenon leads to beneficial enhancements in cementitious materials.

However, nanomaterials tend to agglomerate when introduced into cement paste due to their strong adsorption and Van der Waals forces. This agglomeration challenges achieving the desired enhancement effect and may form areas with compromised structural integrity.

Effective dispersion techniques are necessary to disperse nanomaterials and improve their stability in cement paste in order to solve this problem. The physical dispersion process plays a crucial role in achieving optimal dosage and uniform distribution of nanomaterials during hydration. Simultaneously, the impact of chemical dispersion methods on hydration depends on the specific type and quantity of admixtures used, necessitating careful and comprehensive analysis.

Nanotechnology encompasses various fields that deal with microscopic objects, structures, or materials. Nanomaterials are typically measured in lengths ranging from sub-nanometres to several hundred nanometres. The incorporation of nanoparticles into cementitious materials has been shown to provide significant improvements. This is primarily attributed to the large surface area of nanoparticles, which enhances their chemical reactivity. The increased surface area facilitates the formation of hydration products by providing numerous nucleation sites. This phenomenon leads to beneficial enhancements in cementitious materials (Kishore et al., 2023) Nevertheless, in cement paste, nanomaterials tend to form agglomerates due to their strong adsorption and Van der Waals forces. This agglomeration hinders the desired enhancement effect and can result in forming areas with weakened structural integrity.

Efficient dispersion techniques are necessary to disperse nanomaterials and effectively enhance their stability in cement paste. The physical dispersion process plays a crucial role in achieving optimal dosage and uniform distribution of nanomaterials during hydration. Meanwhile, the impact of chemical dispersion methods on hydration is contingent upon the specific type and quantity of admixtures employed, requiring careful and thorough analysis (He et al., 2023)

In this study, chemical dispersion is done both physically and chemically. We use the Polycarboxylate ether-based superplasticizer for chemical modification of the structure. CBN has incorporated cement sand and water with different methods for mechanical dispersion.

Dry Mixing of CBN – During the initial stage of the mixing process, the dry components, as shown in Figure 3.7 a) comprising cement, sand, and carbon black, are combined and mixed in a mortar mixer for 60 seconds. Following this step, a blend of water and superplasticizer is introduced into the aforementioned dry mixture, consisting of cement, sand, and carbon black. Subsequently, the resulting wet mixture is subjected to an

additional mixing period of 2 minutes. As a result, the flow table shows that the carbon black nanoparticles within the cement matrix undergo agglomeration, thereby indicating an inadequate dispersion of carbon black within the paste. Figure 3.7 b) depicts the structure formed by the agglomeration of carbon black when it interacts with the cement matrix. Subsequently, the prepared mortar mix is cast into moulds to evaluate the compressive strength of the incorporated CBN.

a) **b)**

Figure 3.7 a) Dry Mixing b) Agglomeration After Mixing

Water Mixing – In this particular mixture, the replacement of CBN is set at 0.5%. Initially, the CBN is mixed with water and a superplasticizer, and the resulting mixture is manually stirred using a rod for 3 minutes. Subsequently, a dry mix of sand and cement is introduced into a mortar mixer for 60 seconds to facilitate the incorporation of water into the sand and cement. The dry and nanosuspension mix is combined and mixed for 2 minutes. However, it is observed that during the mixing process of the nanosuspension with the dry mix of cement and sand, a considerable amount of carbon black remains at the bottom of the jar, shown in Figure 3.8, indicating inadequate dispersion of CBN due to improper mixing with water. Afterwards, the prepared mortar is cast into moulds to assess its mechanical properties.

a) b)

Figure 3.8 a) Water mix b) Flow property of water mix

Ultra-Sonication Mixing – Ultrasonication is a common practice dispersion method in nanomaterials. It involves the application of high-frequency sound waves, typically in the ultrasonic range (above 20 kHz), to a liquid medium containing nanomaterials. These forces help break down agglomerates and promote the dispersion of nanoparticles within the liquid. In our study, the dispersion of CBN with a replacement ratio of 0.5% was conducted with a mix having a water-to-cement (W/C) ratio of 0.47. Initially, the superplasticizer was mixed with water and stirred for 2 minutes using a rod. Subsequently, the predetermined amount of CBN was added to the mixture. This suspension was then subjected to ultrasonication for 15 minutes at a frequency of 20 kHz. The beaker containing the suspension was submerged in a water bath to prevent excessive heat generation during the sonication process.

Following the ultrasonication step, the pre-mixed cementitious materials comprising cement powder and silica fume were added to the suspension. The resulting mortar mixture is subsequently poured into oiled moulds and subjected to vibration to eliminate entrapped air bubbles within the paste. However, it has been observed that during the subsequent mixing process of the nanosuspension with the dry mix of cement and sand, a substantial amount of carbon black tends to settle at the bottom of the jar, as seen in Figure 3.9(b). This occurrence indicates inadequate dispersion of CBN due to improper mixing with water.

By employing this methodology, the aim is to achieve a well-dispersed CBN within the cementitious matrix, thereby enhancing the properties of the resulting material.

a)

b)

Figure 3.9 a) Ultrasonication Machine b) Residue left of CB0.5%

Mechanical Mixing. A 10mm half-metal electric drill, as shown in Figure 3.10 was equipped with reverse/forward control to disperse the CBN into an aqueous solution comprising water and a superplasticizer. Carbon Black Nanoparticles (CBN) into an aqueous solution containing water and superplasticizer. The drill operated at 350 watts, 2800 rpm, and -220V. The experimental process began with the uniform dissolution of carbon black in the water and superplasticizer solution. Subsequently, mechanical mixing with the electric drill ensured uniform dispersion of the nanosuspension for 10 minutes. A dry mixing process was then performed using a mortar mixer for 0.5 minutes, incorporating cement and sand components. The nano-cementitious suspension was added to the dry mixture and mixed for five minutes using the mortar mixer. A good mixture obtains, as shown in Figure 3.10(d). Flowability was assessed (Figure 3.10 (f) on the flow table, achieving a 110mm flow as per ASTM1437. Fresh mortar specimens were cast in moulds and subjected to a 7-day curing period for mechanical property evaluation. Notably, this method resulted in negligible residue in the mixing jar compared to other mixing techniques.

a)

b)

c)

d)

e)

f)

Figure 3.10 a) Electric drill b) Mechanical Mix c) Residue Left d) After Mixing e) Flow Specimen f) Flowability of Mortar

3.5.2 Rheological Behaviour

This test method assesses the flow properties of hydraulic cement mortars and mortars containing cementitious materials other than hydraulic types of cement. Although flow is not generally stated in hydraulic cement standards, it is frequently used in standard tests that require the mortar to have a certain amount of water to reach a certain level of flowability.

Procedure followed

As specified in (ASTM, 1437: 2007), the flow table test involves the following sequence of steps:

The flow table must be thoroughly cleaned and dried. Following that, the flow mould is precisely positioned in the centre. An approximately 25 mm thick layer of mortar is then placed in the mould and compacted by tamping it precisely 20 times.

The excess mortar is trimmed to achieve a level surface aligned with the top of the mould using a straightedge or trowel's edge. Without delay, the flow table is dropped 25 times within a 15-second. After the mixing process, the mould is lifted away from the mortar.

The diameter of the mortar is measured along the four marked lines on the table's surface, and the values for each diameter are recorded.

The arrangement of the flow table and the spread of the mortar after 25 blows are depicted in Figure 3.11 (a,b).

Figure 3.11 a) Flow table and b) Specimen for Flowability

3.5.3 Mechanical Properties.

3.5.3.1 Compressive Strength

A compressive strength test was conducted on carbon black nanomaterials mixed mortar with varying CB0 CB1 CB2, and CB3 at normal and targeted temperatures (200,400,600 and 800°C. The specimens were positioned in a compression testing machine, with the

opposite faces of the cast cubes being subjected to the applied load. A continuous load was applied to the specimens at a 0.6 KN/sec rate. Five cubes were cast and subjected to a 28-day curing process for each mixture ratio.. The testing procedure followed the guidelines outlined in the (C. ASTM, 2005) code, while the loading rate was determined according to the (IS 516-1959) standard. The compressive strength was calculated using the prescribed relationship.

$$\text{Compressive Strength} = P/A$$

P = Maximum Load at failure of specimen

A = Area of the contact surface

3.5.3.2 **Flexural Strength**

The flexural strength test was conducted using flexural testing, which comprised two roller supports with a diameter of 10mm. These roller supports were positioned at a span of 100mm. In order to exert the load 'P' on the opposing side of the sample, a third roller with the same diameter was placed at an equal distance from the first two supports represented in Figure 3.12(b). The flexural strength of cement mortar prisms was evaluated by conducting three-point bending tests by the ASTM C348 standard. The prisms used for testing had dimensions of 40 × 40 × 160 mm and were subjected to a loading rate of 0.05 mm/min. The tests were performed on the 28th day of the curing process. In order to study the effects of different replacement percentages (CB0, CB1, CB2, CB3), the prisms were cast using triple-gang moulds, as shown in Figure 3.12(a). Subsequently, the prisms were cured for 28 days in a curing tank to ensure complete hydration of the cement.

a) **b)**

Figure 3.12 a) Triple Gang mold b) Prism Setup

3.6 Residual Mechanical Properties

After a curing period of 28 days, the specimens underwent a heating process in an electric furnace. The furnace interior was equipped with coils to ensure controlled heating. In order to prevent any damage caused by excessively high temperatures surpassing the specified limit, an automatic temperature control panel was utilized to manage the furnace's temperature shown in Figure 3.13.

The specimens were initially exposed to preconditioning by oven-drying at 100±5°C to prepare them for the heating procedure. The specimens were then put inside the electric furnace at 200, 400, 600, and 800°C, the desired temperatures. The heating process within the furnace was controlled by the furnace's built-in thermostat, which maintained a heating rate of 10°C per minute until the desired temperatures were reached. Once the desired temperatures were attained, the specimens remained in the furnace for two hours to ensure uniform heating across their cross-sections. After this period, the furnace's power was switched off. Following a cooling period of 24 hours, the specimens were removed from the furnace and left to naturally cool down in the laboratory until they reached ambient room temperature. Subsequently, a range of experimental tests were conducted on the heated specimens.

Figure 3.13 Electric Furnace

3.6.1 Weight Loss

The weight loss observed in the specimens can be attributed to the evaporation of water at elevated temperatures. Following the completion of the curing period, the specimens underwent preconditioning by subjecting them to a temperature of 100±5°C. Before being placed in the furnace, the weights of the specimens were measured. Subsequently, the

specimens were exposed to targeted temperatures of 200, 400, 600, and 800°C in the furnace. After the high-temperature exposure, the weights of the specimens were measured again. The percentage weight loss was determined by calculating the average mass loss of five specimens at each temperature.

3.6.2 Image analysis (FE-SEM) Field Emission Scanning Electron Microscopy

After performing the mechanical test at normal temperature and elevated temperature, tiny pieces or mortar chunks were extracted from the central region of specimens. In order to facilitate microstructural analysis, these samples were then coated with a layer of gold using sputtering. The sample was analysed using a field emission scanning electron microscope (FE-SEM) Figure 3.14, operating in secondary electron mode. Scanning electron microscopy (FE-SEM), images offer valuable insights into the characteristics of the material, including grain size, shape, porosity, and agglomeration. FE-SEM provides exceptional resolution, a wide magnification range, and a significant depth of field, making it a powerful tool for detailed examination and analysis. An SEM was used to capture images of the samples, and an EDS analyser was used to ascertain any variations in the elemental composition within the boundaries of the captured images.

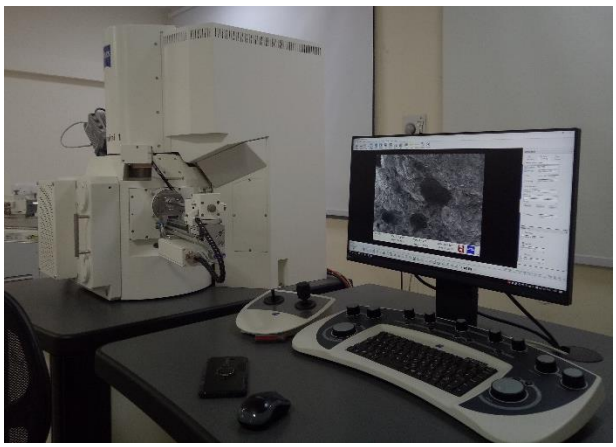

Figure 3.14 SEM Operating System

3.6.3 X-ray- Diffraction

The XRD patterns of Carbon black nanoparticles incorporated mortar were acquired using a Bruker X-ray diffractometer employing CuKα radiation in the 2θ = 5-55 range. Powdered mortar mixes were examined before and after exposure to high temperatures, following a sieving process using a 100 μm sieve. The identification of crystalline phases within the mortar samples was accomplished by analyzing the XRD patterns obtained

from an X-ray diffractometer (Xpert Pro, PAN analytical) that utilized Cu Ka radiation with a wavelength of $\lambda = 1.54$ Å. The XRD patterns of Carbon black nanoparticles were recorded within a 2θ angle range spanning from 10 to 90°. X-ray diffraction is the predominant technique for studying the structural characteristics of materials in thin film formats.

Chapter 4

Result And Discussion

4.1 General

The central objective of this research is to synthesize Carbon Based Nanomaterials that are stabilized with superplasticizer and investigate their influence on the physical, mechanical, and chemical properties of pure cementitious nanocomposites as well as CBN-blended cementitious nanocomposites. The study focuses on evaluating the behavior of these materials under high-temperature conditions, aiming to gain insights into their performance in challenging environments. By achieving this, the research aims to contribute to a comprehensive understanding of the material's response to demanding thermal conditions.

A Polycarboxylate ether-based superplasticizer (PCE) was employed to stabilize the CBN to achieve better dispersion in the cement pore solution. Chapter 1 outlines the background of the study, while Chapter 3 presents a detailed experimental methodology to meet these objectives. The results and discussion from the investigation are systematically analyzed. Figure 4.1 provides an overview of the main structure of the results and discussion.

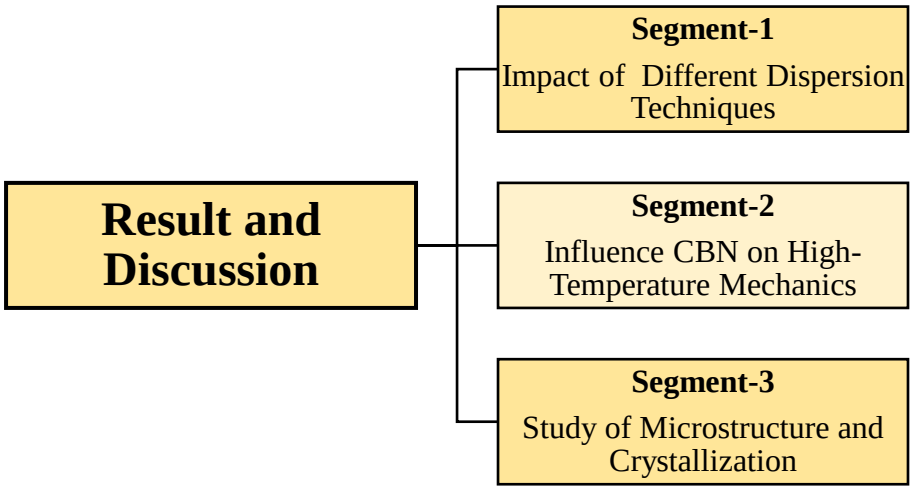

Figure 4.1 Schematic Interpretation of Result and Discussion

4.2 Effect of Dispersion Methods on Workability of Carbon Black Nanoparticles in Cementitious Materials

The workability of carbon black nanoparticles was examined using various dispersion methods, and the rheological properties of cementitious materials were assessed using the flow table test. Figure 4.2 displays the mini-slump results obtained from different dispersion methods. Mechanical mixing (MM) demonstrated effective dispersion when combined with 0.4% superplasticizer (SP), resulting in a mini-slump of 115mm by ASTM1437 standards. Conversely, other dispersion methods showed limitations; in some cases, the slump broke during 25 blows, and agglomeration occurred in the fresh mixture shown in Figure 4.2.

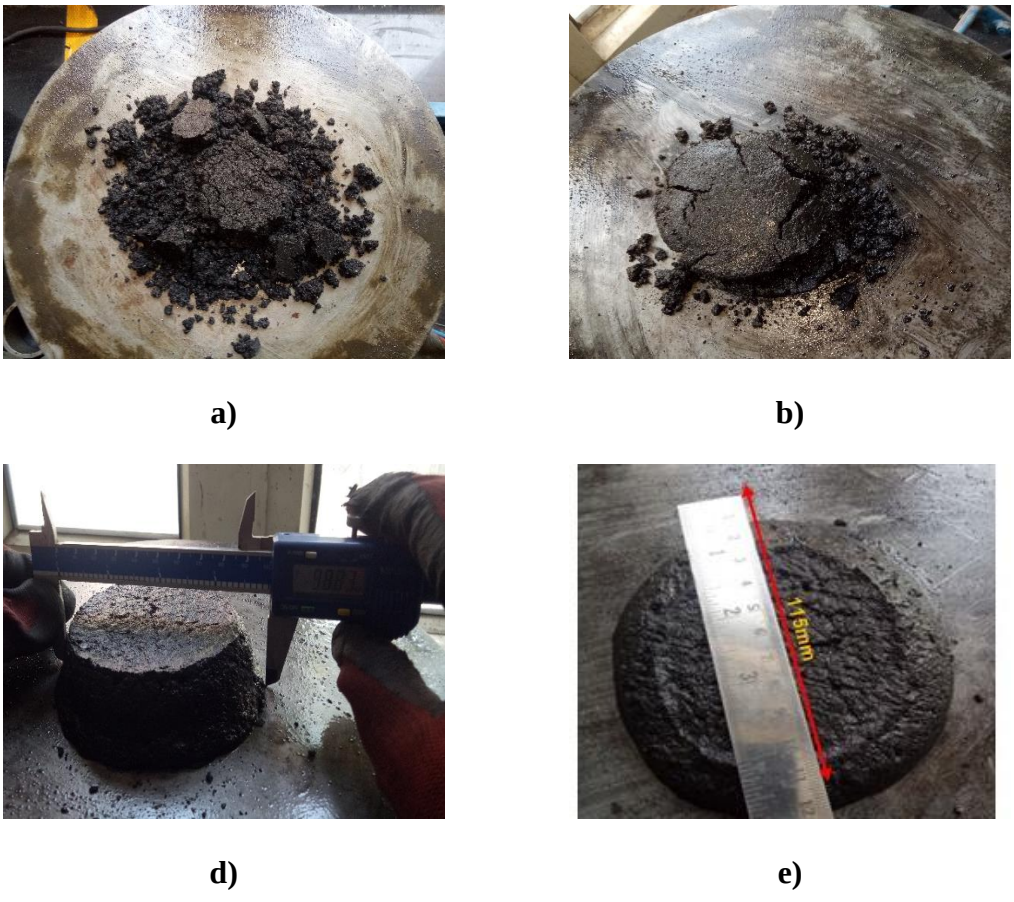

Figure 4.2 a) Dry Mixing b) Water Mixing c) Ultrasonication Mixing d) Mechanical Mixing

Ultrasonication provided a better fluidity with a slump of 97mm; however, the residue remaining after sonication mixing was higher than mechanical mixing. As a result, the Ultrasonication method was not considered suitable for achieving the desired dispersion. Based on these findings, mechanical mixing with superplasticizer supplementation was

selected as the optimal dispersion method for carbon black nanoparticles in cementitious materials. It is noteworthy that polycarboxylate superplasticizers are considered highly effective dispersing agents, outperforming other surfactants in nanoparticle applications (Korayem et al., 2017).

4.3 Effect on Mechanical Strength of Different Dispersion methods

The seven days' compressive strength results for various dispersion methods are illustrated in Figure 4.3 For the trial mix, a carbon black nanomaterial dosage of 0.5% by mass of cement and 0.3% of superplasticizer were utilized. The graph denotations are as follows: DM for dry mix, US for ultrasonication, WM for water mix, and MM for mechanical mix. Remarkably, the mechanical mixing method (MM) exhibited superior performance in terms of compressive strength after the 7-day curing period. The strength increased by 22.73% compared to the dry mix and by 8% in comparison to the ultrasonication method. This notable enhancement in strength is attributed to the more effective dispersion of carbon black nanoparticles within the mortar samples.

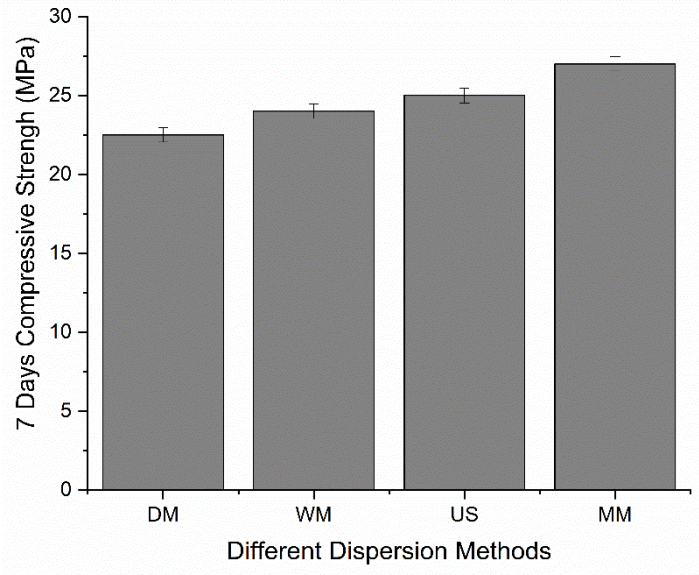

Figure 4.3 7 Days Compressive Strength of Different Dispersion Methods

4.4 Impact of carbon black nanoparticles on workability of cement paste

Figure 4.54 presents the mini-slump diameters of CB0, CB1, CB2, and CB3. With an increase in the content of Carbon black nanoparticles, the mini-slump diameter decreases. Mainly, CB3% exhibits a notable decline in fluidity due to CB's significantly higher specific surface area than plain cement paste. The mini-slump flow test highlights the

cement paste's reduced workability upon adding carbon black nanoparticles. These findings align with (Zhang et al., 2022)previous research, which reported a decrease in fluidity when incorporating CBN in cement paste, attributed to the distinct tendency of Carbon black (CB) to absorb substantial quantities of free water during the stirring phase of fresh mortar. The higher proportion of finer particles facilitated better particle packing, reducing voids within the cement matrix. As a result, the space available for water to bleed over the mortar surface decreased. Consequently, the stiffness of the mortar increased, and its flowability decreased.

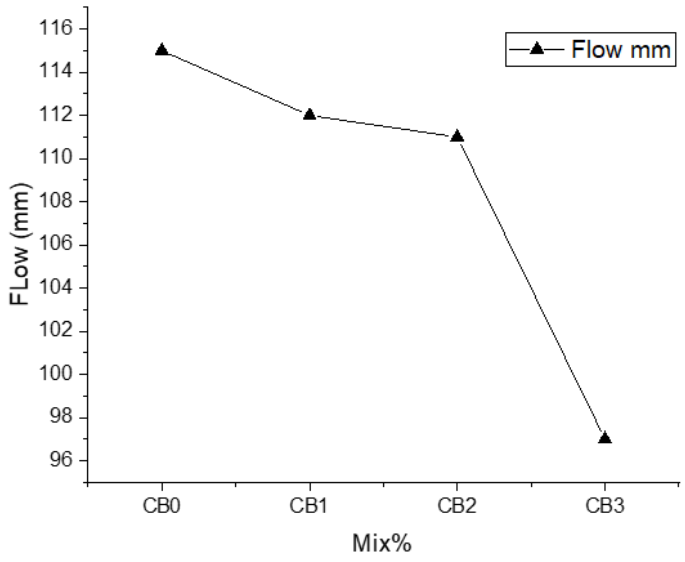

Figure 4.4 Influence of CB Content on Fluidity of Cementitious Specimens

4.5 Effect of Mechanical mixing on 7 days Compressive Strength

After selecting the mechanical mixing method as the final dispersion technique, the dosages of carbon black nanoparticles were determined based on a comprehensive literature review and various trial mixes, considering their flowability. In Figure 4.5, CB represents Carbon black nanomaterial, and 0 denotes the control specimen, while 1, 2, and 3 represent the replacement ratios of carbon black with cement. After 7 days of curing, the compressive strength results indicated that the 3% CB dosage exhibited the highest strength, with a significant increase of 22.7% compared to the control sample. Additionally, CB2% demonstrated an 8.7% strength increment compared to CB1%.

Compared to the control specimen, these enhancements can be attributed to the dense microstructure of carbon black particles in the mortar. Moreover, the effective dispersion of CB3% within the cement matrix contributed to its superior strength compared to other carbon black incorporated samples.

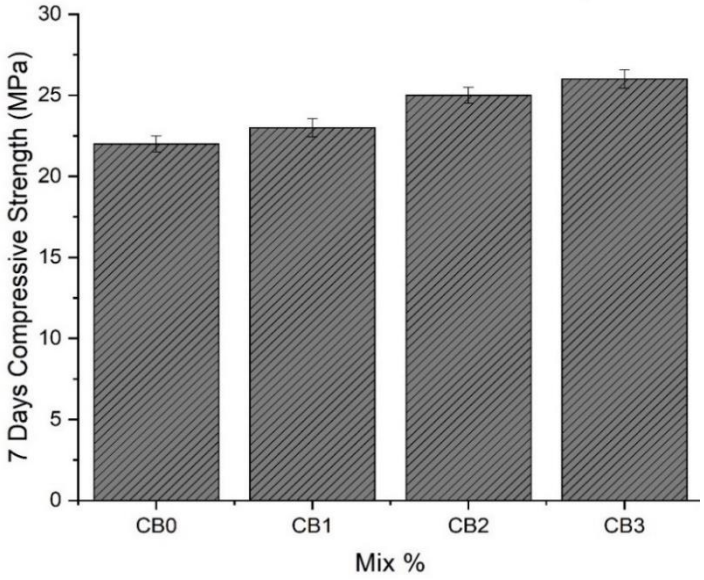

Figure 4.5 Seven-day compressive strength of finalized selected mix used for current study

4.6 Effect of CBN on mechanical properties

4.6.1 Compressive Strength

After a 28-day curing period, the specimens were subjected to compressive strength and flexural strength tests. Figure 4.6 illustrates the evaluation of compressive strength properties. The addition of CBN in varying dosages led to notable improvements in the compressive strength of mortar, showing a clear enhancement trend. The mortar's compressive strength achieved peak values at CBN dosages of 1%, 2%, and 3%, measuring 28.60 MPa, 29.80 MPa, and 32 MPa, respectively. Compared to the control group, the compressive strength values for the mortar with CBN dosages of 1%, 2%, and 3% were 0.35%, 3.5%, and 4.1% higher. This enhancement in compressive strength is attributed to the filler effect of CBN, whereby it fills the pores and capillaries of the matrix, resulting in increased strength (Rezania et al., 2019)

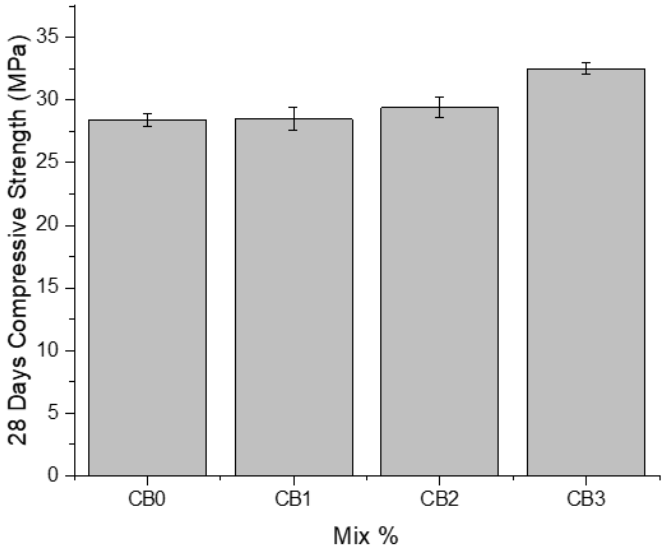

Figure 4.6 28 Day Compressive Strength of CBN

4.6.2 Flexural Strength

The flexural strength results after 28 days of curing are depicted in Figure 4.7 Incorporating CBN in the cementitious matrix influences the strength decrement, leading to a decrease compared to the control specimens. Notably, the control specimen, devoid of CBN, exhibits the highest flexural strength of 8.32 MPa, surpassing the strength values of the other CBN dosages. Specifically, CB1 demonstrates a strength decrement of 21.87%, CB2 exhibits a 12.86% reduction, and CB3 shows an 8.6% decrease compared to the control cement paste. This decline in strength suggests the inherently brittle nature of CBN.

Similar findings were reported by (Zhang et al., 2022) in their previous studies, supporting the observation of reduced strength with CBN inclusion. The decreased flexural strength in CBN-incorporated specimens indicates the complex interaction of nanoparticles with the cementitious matrix, affecting the cohesion and interlocking of fibrous phases, such as CSH single bonds and needle-like ettringite (AFm), which are crucial for strength development. Further research is warranted to comprehend the specific mechanisms governing the impact of CBN on the flexural behavior of cementitious composites. Moreover, (Li & Li, 2019) conducted a related study, concluding that the presence of CB nanoparticles may function as a lubricant, weakening the bond between aggregates and the cementitious binder. As a result, the effectiveness

of aggregate bridging at the crack tip could be compromised, facilitating the propagation of cracks.

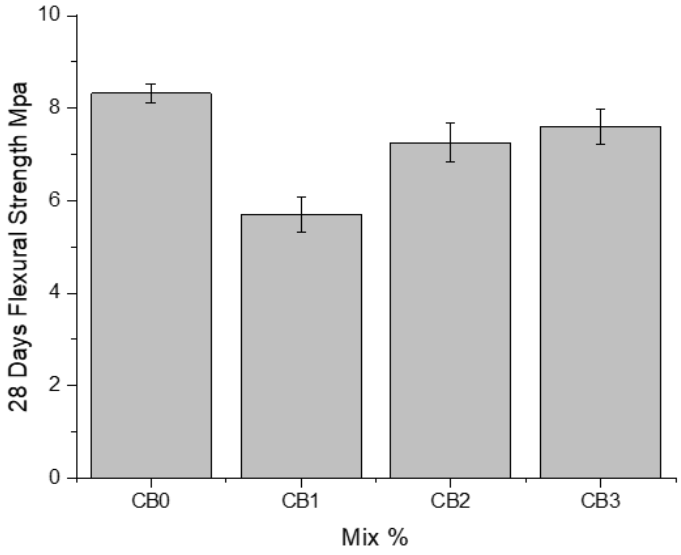

Figure 4.7 Flexural Strength Variation After 28 Days

4.7 Effect of Targeted Temperatures on the Properties

4.7.1 Colour Change

The visual appearance of all samples was documented at room temperature 25°C and after exposure to 200°C, 400°C, 600°C and 800°C Figure 4.8 pronounced colour changes were evident in all nanoengineered cementitious mortar samples, particularly following exposure to 600°C and 800°C of high-temperature effects. While the CBN mortar samples were dark grey at room temperature, shown in Figure 4.8(a), they exhibited a light grey, especially after being subjected to 800°C- Notably, no breakage, fragmentation, disintegration, or chipping were observed in any of the CBN mortar samples compared to the control specimens.

At 600°C, the CBN underwent partial combustion, turning its exterior from dark black to light grey. However, upon closer examination, a dark black patch was observed in the centre of the specimens, indicating that the CBN was not entirely converted into ashes, and a portion remained inside the specimens. At 800°C, even less residue of burnt CBN was observed compared to the targeted temperature of 600°C.

Furthermore, the impact of replacing Carbon black nanoparticles is evident in the burnt residue of CBN at 600°C and 800°C temperatures. The degree of replacement influences

the extent of the observed black patches, as depicted in Figure 4.9. These observations were specifically evident within the temperature range of 600-800°C. The surface colour changes observed in the specimens provide valuable insights into the potential mechanisms underlying damage and offer a comprehensive guideline for determining the temperature exposure of specific structures (Kodur, 2014).

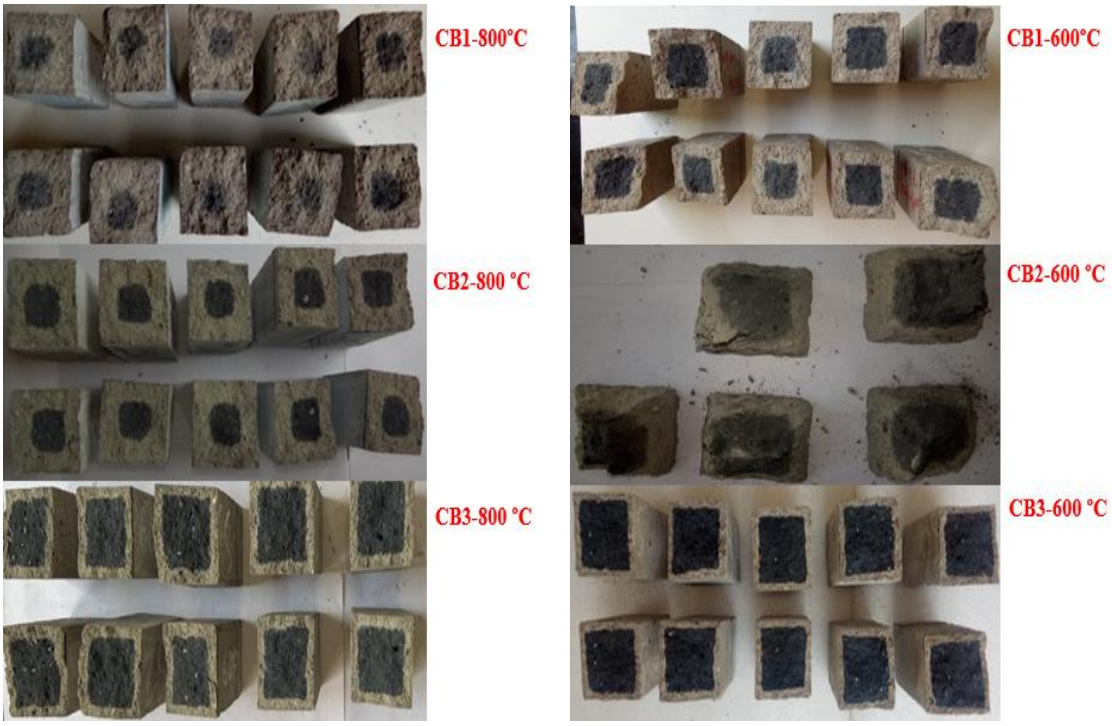

Figure 4.8 Residue left Inside the CBN specimens at a) 800°C and b) 600°C

a)

b)

c)

d)

e)

Figure 4.9 Surface colour appearance before and after at different temperatures a) 200°C b) 400°C c) 600°C d) 800°C

4.7.2 Residual Compressive Strength

The impact of high temperatures on the compressive strength of nano-cementitious composites is examined in this study. The study involved evaluating the average residual compressive strength of the mixes using five specimens for each mix and at different temperature levels (200, 400, 600, and 800 °C). Upon exposure to 800°C, the nano cementitious composites experienced a decrease in compressive strength, resulting in increased material brittleness. Figure 4.10 illustrates the impact of elevated temperature heat treatment on the remaining compressive strength of the specimens.

At 200°C, the compressive strength slightly increased for all specimens incorporated with Carbon black nanoparticles (CBN) or without CBN.

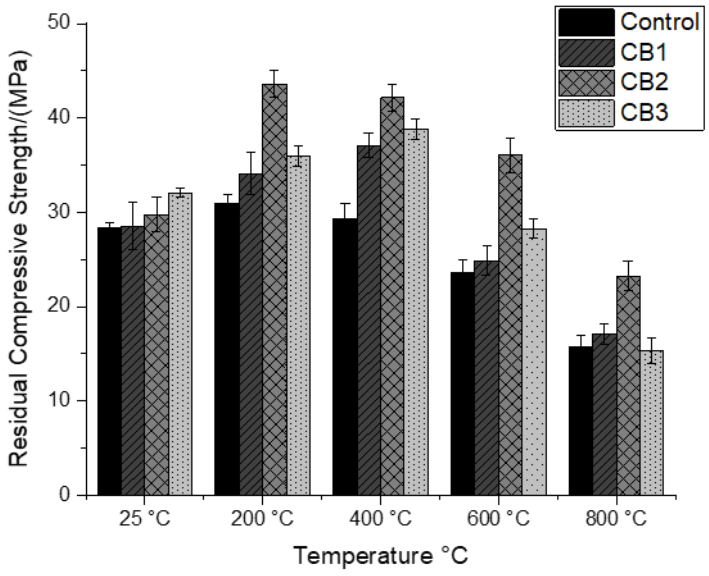

Figure 4.10 Residual Compressive Strength for different samples

However, the specimens' residual compressive strength declined with further temperature increases. For instance, at 200°C, specimens containing 0% CBN (control), 1%, 2%, and 3% CBN demonstrated increases in compressive strength of 9.15%, 19.30%, 46%, and 12%, respectively, compared to their mix tested at room temperature. This enhancement in strength can be attributed to the increased hydration of anhydrous cement grains facilitated by an internal autoclaving reaction. Additionally, the formation of extra hydration products filled the pores, further enhancing compressive strength at 200°C. These findings are consistent with those reported by, (Amin et al., 2015; Han et al., 2022b). Notably, at 200°C, CB2 exhibited the highest compressive strength of 43.62 MPa compared to the other specimens.

After exposure to 400°C, all the specimens exhibited a decrement in compressive strength compared to the targeted temperature of 200°C. The de-hydroxylation of portlandite at 400°C led to an increase in porosity within the cement matrix structure, as confirmed by the study conducted by (Moosavi et al., 2019) In this temperature range, the specimen without incorporating Carbon black nanoparticles (CBN) experienced decreased strength. Conversely, the specimens with different CBN dosages showed an increment in strength by 32%, 44.8%, and 12% (Figure 4.11), respectively, compared to the mix strength tested at room temperature.

This enhancement in strength can be attributed to the finer particles of CBN contributing to the formation of a dense microstructure within the cement matrix, acting as a filler. Among the CBN dosages, CB2 exhibited the highest strength of 42.15 MPa at 400°C compared to the other mixes incorporated with CBN dosages.

The reduction in compressive strength at temperatures ranging from 600 to 800°C is illustrated in Figure 4.10. Among the different Carbon black (CB) dosages, CB2 exhibits negligible strength reduction at 600 and 800°C. At 600°C, the breaking of CSH gel commences, while at 800°C, the complete deterioration of CSH gel leads to the formation of cracks and voids, resulting in decreased specimen strength. This phenomenon has been previously observed in studies conducted by (Liang et al., 2019).

Notably, at 600°C, CB2 demonstrates a minimal loss in strength, retaining a strength value of 36 MPa. Moreover, at the targeted temperature of 800°C, the control specimen exhibits the highest loss in strength compared to other mixes, while CB2 exhibits the maximum strength retention at 23.24 MPa. These findings demonstrate the favourable results of CB2 in terms of residual compressive strength at different targeted temperatures. This study provides valuable insights into the behavior of cementitious composites containing CB at elevated temperatures and contributes to understanding their potential applications in various engineering fields.

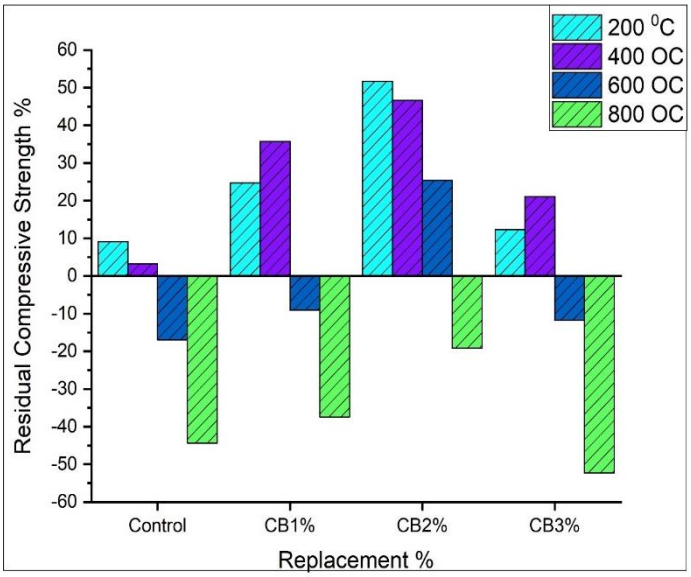

Figure 4.11 Reduction in Strength at high temperatures

4.7.3 Residual Flexural Strength

The residual flexural carrying capacity of the prisms is depicted in Figure 4.12. At 200°C, there is an increment in the flexural strength of the prisms compared to their strength at normal temperature. CB2 exhibits the highest flexural strength of 11.3 MPa at 200°C, surpassing the other mixes. Control, CB1, and CB3 show strength increments of 30.83%, 55.53%, and 20.2%, respectively, concerning their strength at normal temperatures.

At 400°C, CB2 and CB3 show enhancements in strength compared to the control specimens. Additionally, CB2 and CB3 demonstrate beneficial effects with strength enhancements of 8.6% and 4.7%, respectively, relative to their strength at normal temperatures. This increase in strength can be attributed to the filler nature of CBN, which contributes to the formation of a dense microstructure with fewer voids, thereby delaying the formation of cracks.

However, from 600 to 800°C, the flexural strength gradually decreases due to the complete breakdown of CSH and the onset of decarbonization, leading to a deterioration in strength. At 800°C, CB2 exhibits good strength of 3.62 MPa compared to the other mixes incorporated with CBN and without CBN. Overall, the results demonstrate CBN's effect on the specimens' flexural strength at different elevated temperatures.

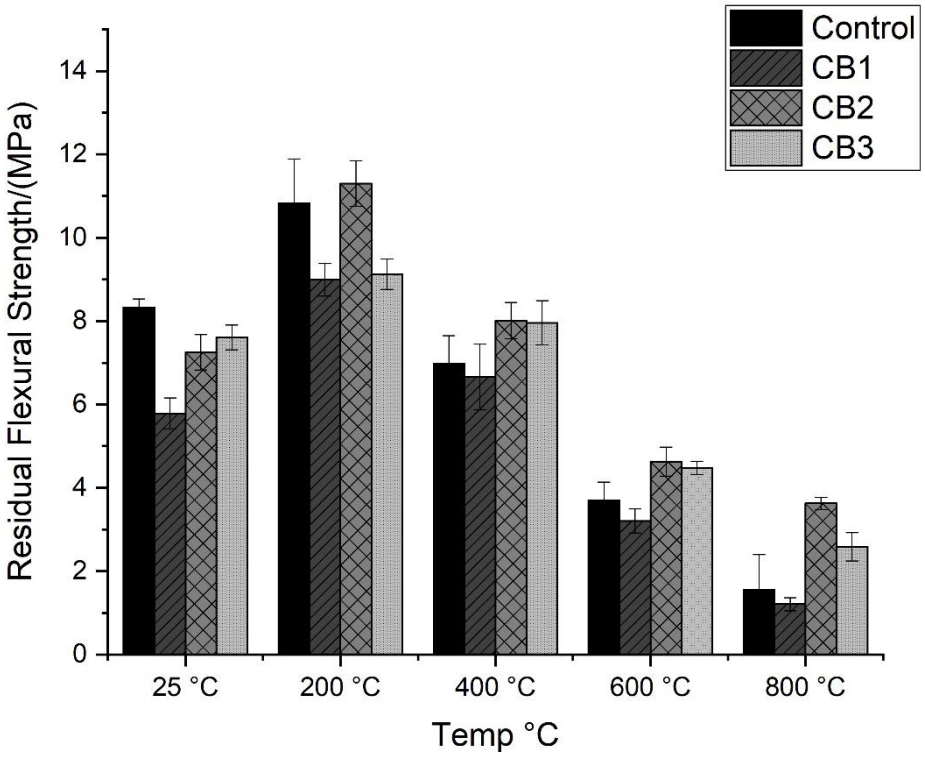

Figure 4.12 Residual Flexural Strength

4.8 Mass Loss

The current study aimed to determine how exposure to fire in the 200°C to 800°C temperature range might affect monolithic and composite samples. Figure 4.13 compares the initial mass at room temperature (25°C) to the mass measured after exposure to various temperatures, with the mass loss data given as a normalised percentage.

The results obtained from Figure 4.13 clearly demonstrate an increasing trend in mass losses for all samples with rising temperatures, indicating the notable effect of high temperatures on the specimens. Further analysis revealed that the main cause of this phenomenon was the dehydration of the mortar samples, attributed to the evaporation of water contained in the alkali activators within the matrix at elevated temperatures.

Among the composite samples, it was observed that at 200°C, a maximum mass loss of below 3% was recorded. This was primarily attributed to the evaporation of physically bound water, resulting in moisture loss from the samples. It indicates that the composite mixtures possess good stability at this temperature range, which is favourable for applications in fire-exposed environments.

However, as the temperature increased further, the mass losses in the composite samples also escalated. At 800°C, the control specimen exhibited the highest mass loss, indicating its susceptibility to elevated temperatures. Remarkably, CB2 demonstrated the minimum mass loss of 2.77% after exposure to 800°C, signifying more stable hydrates than other mixtures.

The observed correlation between the mass loss data and the residual compressive strength of CB2 at targeted temperatures further confirms the significance of stable hydrates in enhancing the material's performance under fire exposure.

Overall, these findi ngs provide valuable insights into the behavior of monolithic and composite samples under high-temperature conditions, shedding light on the material's resilience and potential applications in fire-prone environments.

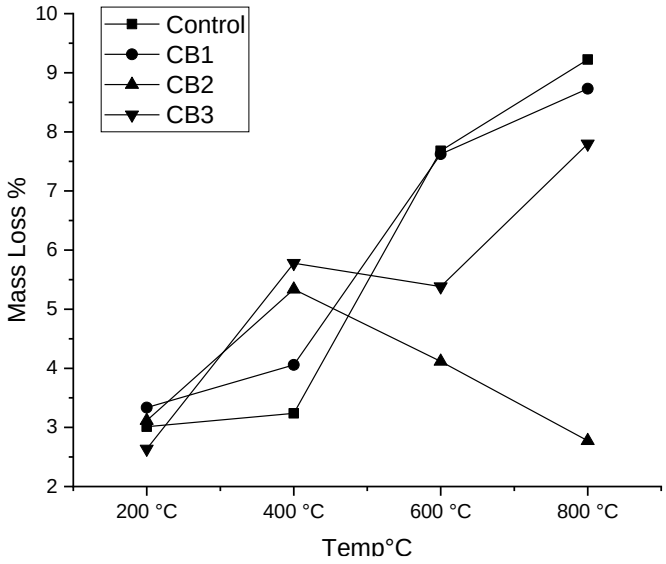

Figure 4.13 Mass Loss at various temperatures

4.9 XRD (X-ray diffraction)

The mineralogical characteristics of the produced mortar mixes were carefully examined using X-ray diffraction (XRD) analysis conducted with the Xpert 3 PAN analytical model diffractometer. The findings of the XRD examination, which was particularly performed on the 28-day water-cured mortar mixes, are shown in Figure 4.14. The graph presents intensity counts on the y-axis and 2 Theta angles on the x-axis. The various mineralogical phases present in the mortar mixes were identified by comparing the obtained data with the JCPDS XRD data file.

The major phases observed in the mortar include portlandite, quartz, and calcium silicate hydrate. The mineralogical composition of the mortar significantly influences its strength and durability. The calcium silicate phase was observed in all the mortar mixes, corresponding to the tri-calcium silicate (C_3S) in the cement. The early age strength of the mortar is primarily attributed to the hydration of C_3S. Moreover, the calcium silicate phase was found in the cementitious composite mortar mixes, with only minimal traces detected in the control mix.

As a result, this calcium silicate phase may be responsible for the carbon black mortar mixes at early age strength. Calcium silicate hydrate (CSH) gel in all the CBN cementitious composite mortar mixes is indicated by another crucial phase for strength development. The presence of CSH suggests the occurrence of hydration reactions and the formation of stable hydration products.

Furthermore, the XRD pattern of the mortar mixes revealed the presence of quartz peaks originating from the inert aggregates used in the composition. These findings provide valuable insights into the mineralogical composition of the mortar mixes and their direct impact on the strength and performance of the materials. The presence of portlandite is evident in all the XRD patterns; however, a reduction in the portlandite phases suggests the consumption of calcium hydroxide (CH) during the process, leading to the formation of secondary hydration products.

The XRD patterns of the nanoengineered cementitious composites, exposed to different temperatures, are depicted in Figure 4.14 (a),b),c) and d)). Notably, the patterns reveal an enhanced presence of portlandite phases at 200°C, indicating the thermal activation of nanocarbon black particles in the mortar. However, the 200°C temperature exposure kept the other mineralogical phases relatively unaffected. Upon exposure to 400°C, the XRD patterns exhibited the disintegration of portlandite, resulting in the release of bound water from the -CH and CSH phases. Meanwhile, the quartz phase mainly remained unaffected in all the mixes. Subsequent exposure to 600°C and 800°C (Figure 4.14 a,b,c,d) displayed primarily the quartz peak.

The findings indicate that including small amounts of CBN in the mortar improved the cement hydration process, increasing compressive strength and stiffness. As portlandite is a by-product of cement hydration, enhanced portlandite levels suggest that

incorporating CBN positively influenced the hydration reaction, improving the mortar's mechanical properties (Lima et al., 2021) Based on the XRD results, the reduction in the mortar's strength is attributed to the loss in the crystal structure of all the hydrated phases, including CH and CSH crystals.

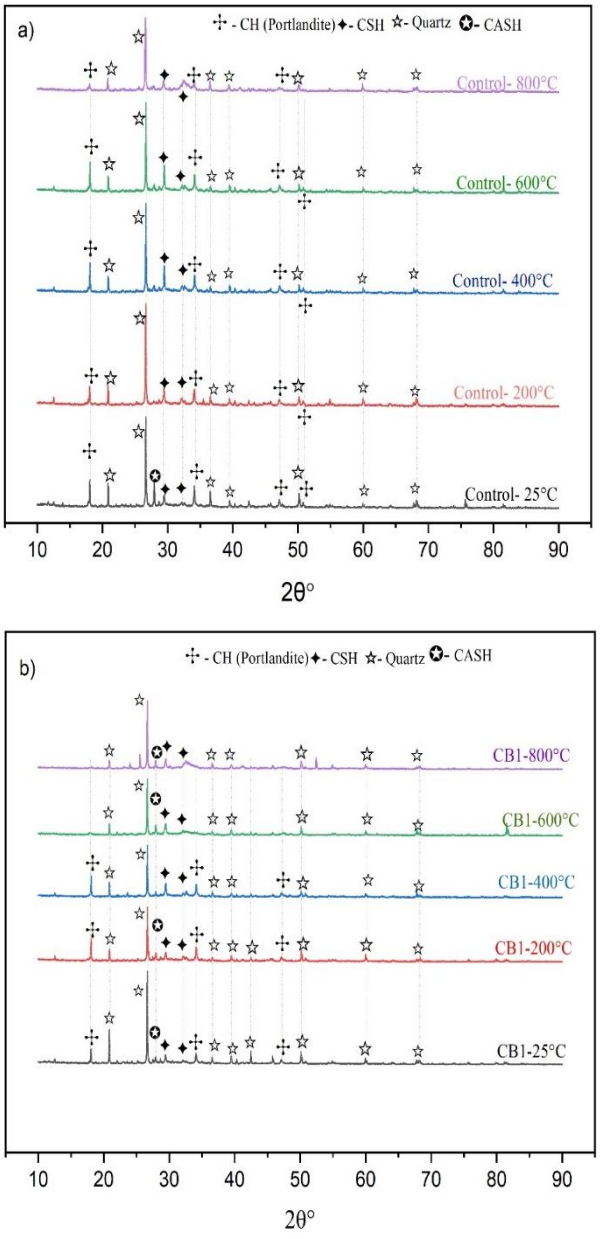

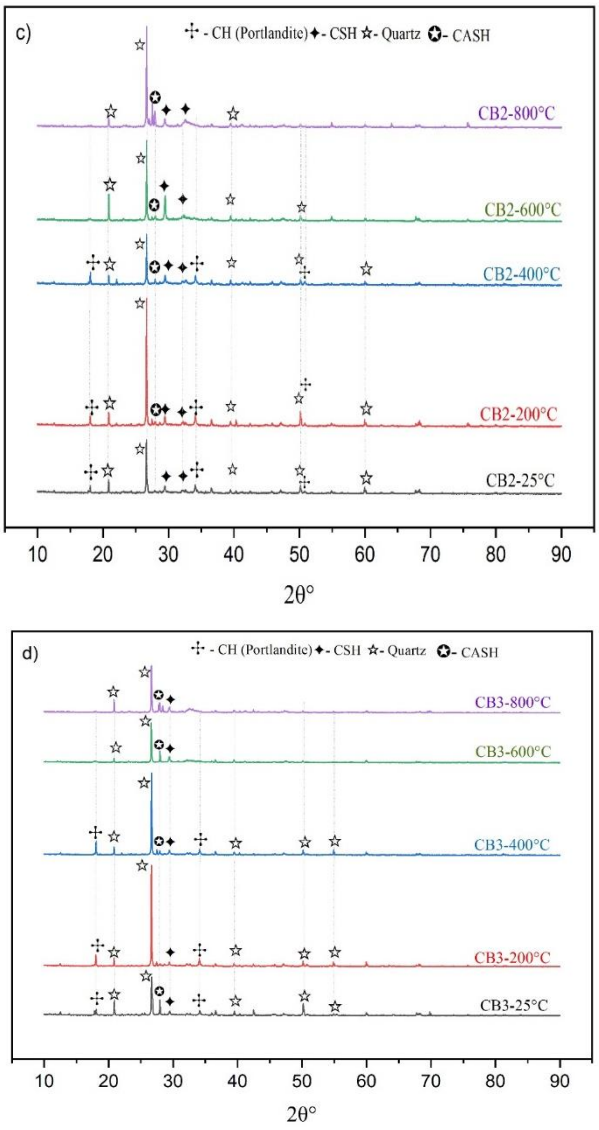

Figure 4.14 XRD Analysis at targeted temperatures a) Control b) CB1 c) CB2 d) CB3

4.10 FESEM (Field Emission Scanning Electron Microscopy)

The FE-SEM images of the nanoengineered cementitious mortars at ambient temperatures and different temperatures are depicted in Figure 4.16. Visual examination of the mortar specimens at increasing temperatures revealed noticeable color transformations, turning grey at approximately 800°C, indicating physical changes in the mortar. The CBN on the mortar surface partially transformed into ashes but remained unburnt. The dark regions observed in the FE-SEM images represent the pores within the mortar.

Comparing the FE-SEM images of the nanoengineered cementitious composites with the normal mortar Figure 4.15, a reduction in dark regions is evident, signifying a significant decrease in the number and volume of pores in the nanoengineered cementitious composites compared to the control mortar. This reduction in pores is likely due to the filling effect of the CBN. Moreover, the presence of CSH gel is evident in the flaky layers observed in the mortar images. The gel-like structure is visibly present at the interface between the CBN and aggregates, enhancing the bonding characteristics of the cement paste. The reinforced interfacial transition zone, facilitated by the improved CSH gel structure, contributed to a notable reduction in capillary pores within the mortar.

Additionally, the FE-SEM images of the CBN mortar mixes reveal well-bonded aggregates with the cement paste, and CBN demonstrates uniform distribution throughout the cement matrix. The incorporation of CBN contributed to the increased denseness of the nano-cementitious mortar, as observed in the FE-SEM images.

FE-SEM analysis of samples exposed to 400°C showed significant changes in the microstructure of pastes without nanofillers, with unclear C-S-H crystals and small micro-cracks. At 600 °C, samples without nanofillers exhibited further changes, including increased voids, micro-cracks, and disrupted C-S-H crystals. However, samples with carbon nanofillers did not show a similar formation of voids and micro-cracks, and some hydrates remained stable after exposure to 600 °C, explaining their higher values of average relative residual strength factors. At 800°C, mortar mix without CBN experiences more voids and cracks than the mortar mix with CBN incorporation. CB2% shows less void and crack structure at elevated temperatures than the control specimens. The presence of more CH-stable hydrate was confirmed through SEM studies. These findings are confirmed by (Nalon, Ribeiro, de Araújo, et al., 2021)

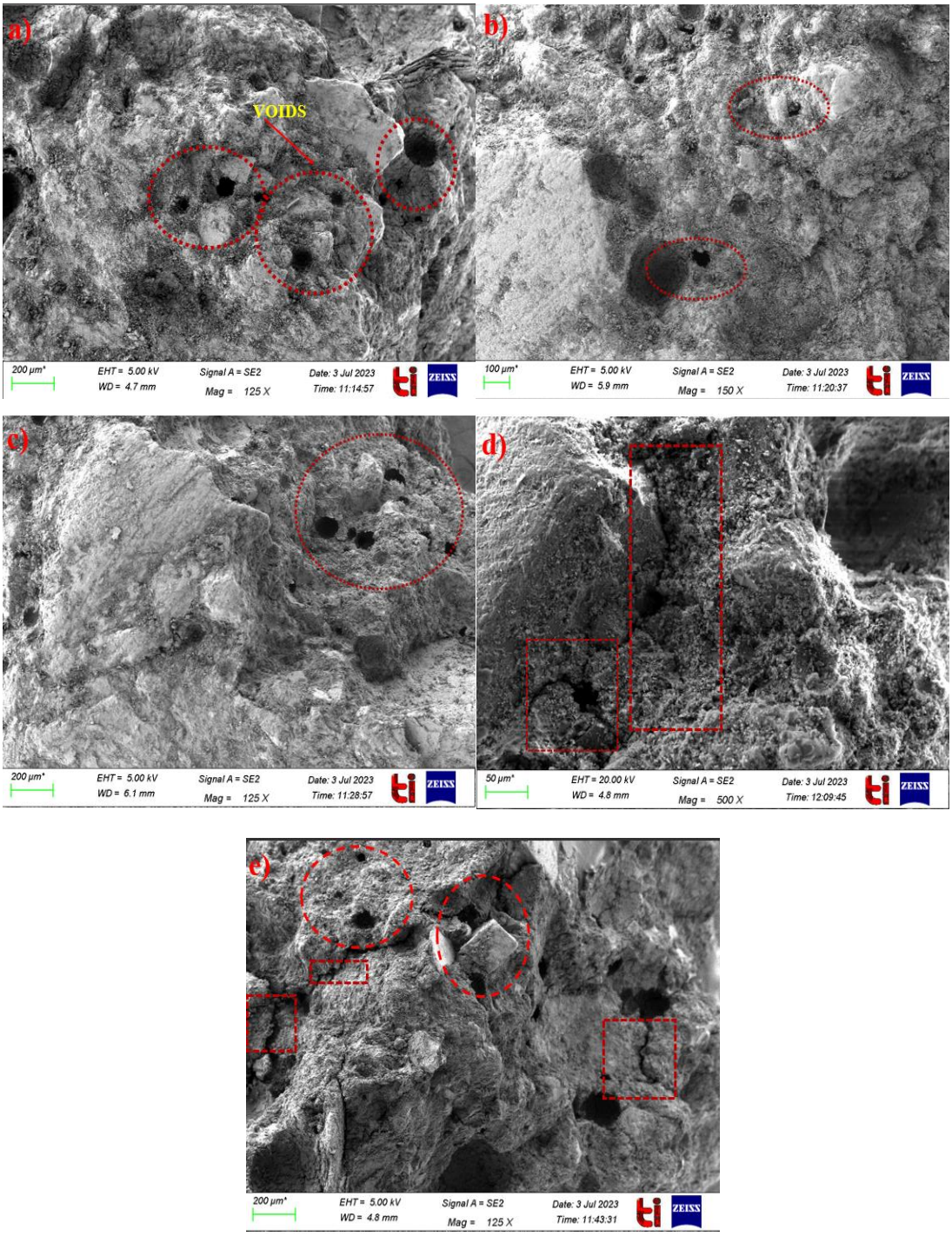

Figure 4.15 SEM Image of Control Mix at different temperature a) Control 25°C b) Control 200°C c) Control 400°C d) Control 600°C e) Control 800°C

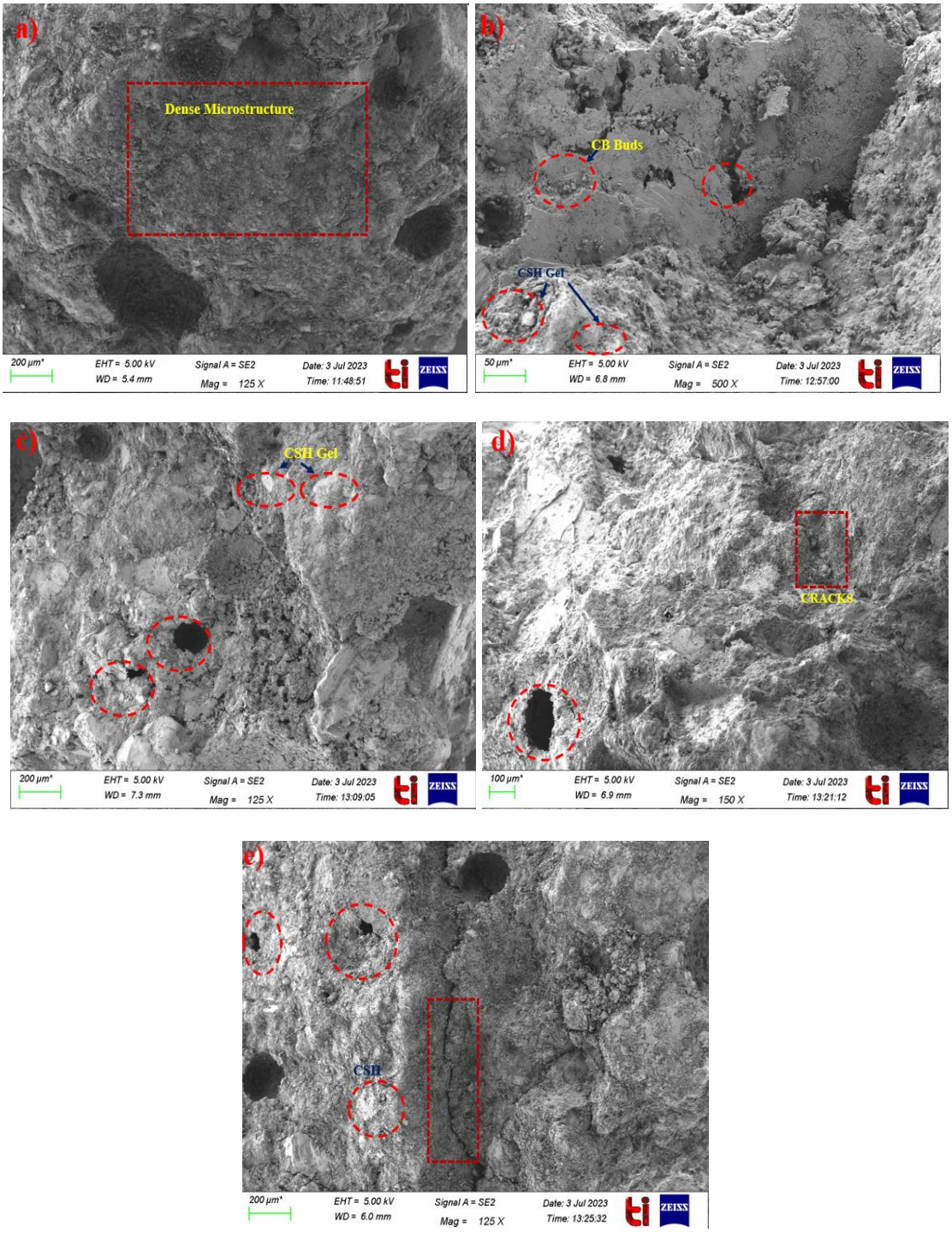

Figure 4.16 SEM Image of nanoengineered composite mix at different temperature a) CB2 25°C b) CB2 200°C c) CB2l 400°C d) CB2 600°C e) CB2 800°C

Chapter 5

Conclusion

In this study, a series of experiments were conducted to comprehensively explore the influence of elevated temperatures and normal temperatures on the mechanical and rheological properties of nanoengineered cementitious composite mortars. These novel mortars were formulated explicitly by incorporating Carbon-Based Nanomaterial (CBN) substitutes, adding to their potential for improved performance in various applications. This study aimed to gain valuable insights into their behavior and response under both regular and extreme thermal environments by subjecting these materials to different temperature conditions. Following conclusions can be drawn from the presented study:

.

- In rheological properties increasing carbon black content decreases workability in nano cementitious composites due to high water absorption during mixing. CB3 significantly affects fluidity due to its higher surface area.
- CBN dosages enhance mortar compressive strength, peaking at 3% replacement (32 MPa). Filler effect of CBN fills pores in mortar, contributing to enhanced strength.
- CBN addition reduces flexural strength due to its inherent brittleness. Control specimen shows the highest flexural strength.
- Exposure to 600°C and 800°C causes CBN appearance changes, indicating temperature-induced damage with cracks and spongy spaces. Valuable insights for structural durability assessment.
- CBN improves compressive strength at 200°C but decreases at higher temperatures. CB2 dosage enhances dense structure and hydrates stability at 600°C and 800°C. Similar performance has been observed in case of flexural strength.
- Mass losses increase with higher temperatures due to mortar dehydration. CB2 shows superior stability after 400°C for fire-exposed environments.
- Mineralogical analysis (XRD) and Micro-structural investigation (FE-SEM), of CB2 with CBN confirms that CB improves mineralogical composition, cement hydration, and enhances residual compressive strength of mortar.

5.1 Future Scope of work

Future research should explore carbon black nanoparticles' potential as a cement alternative in concrete for improved nanoengineered composite properties and fire resistance. Investigations on varying nanoparticle compositions and elevated temperature effects are necessary to fully understand their role in enhancing concrete performance in the construction industry.

Chapter 6

REFRENCES

Afzal, A., Kausar, A., & Siddiq, M. (2016). Perspectives of Polystyrene Composite with Fullerene, Carbon Black, Graphene, and Carbon Nanotube: A Review. *Polymer-Plastics Technology and Engineering*, *55*(18), 1988–2011. https://doi.org/10.1080/03602559.2016.1185632

Alhamad, A., Yehia, S., Lublóy, É., & Elchalakani, M. (2022). Performance of Different Concrete Types Exposed to Elevated Temperatures: A Review. *Materials*, *15*(14), 5032. https://doi.org/10.3390/ma15145032

Amin, M. S., El-Gamal, S. M. A., & Hashem, F. S. (2015). Fire resistance and mechanical properties of carbon nanotubes – clay bricks wastes (Homra) composites cement. *Construction and Building Materials*, *98*, 237–249. https://doi.org/10.1016/j.conbuildmat.2015.08.074

Anwar, A., Liu, X., & Zhang, L. (2023). Nano-cementitious composites modified with Graphene Oxide – a review. *Thin-Walled Structures*, *183*, 110326. https://doi.org/10.1016/j.tws.2022.110326

ASTM, A. (2005). ASTM C494: Standard specification for chemical admixtures for concrete. *West Conshohocken, PA, USA: ASTM*.

ASTM, C. (2005). 109/C 109M-02. *Standard Test Method for Compressive Strength of Hydraulic Cement Mortars (Using 2-in. or [50-Mm] Cube Specimens)*.

ASTM, C. (2007). Standard test method for flow of hydraulic cement mortar. *C1437*.

ASTM C348-18: Standard Test Method for Flexural Strength of Hydraulic-Cement Mortars. *Annual Book of ASTM Standards*, *98*.

Baloch, W. L., Khushnood, R. A., Memon, S. A., Ahmed, W., & Ahmad, S. (2018). Effect of Elevated Temperatures on Mechanical Performance of Normal and Lightweight Concretes Reinforced with Carbon Nanotubes. *Fire Technology*, *54*(5), 1331–1367. https://doi.org/10.1007/s10694-018-0733-z

Baomin, W., & Shuang, D. (2019). Effect and mechanism of graphene nanoplatelets on hydration reaction, mechanical properties and microstructure of cement

composites. *Construction and Building Materials*, *228*, 116720. https://doi.org/10.1016/j.conbuildmat.2019.116720

Bera, M., Gupta, P., & Maji, P. K. (2019). *Structural/Load-Bearing Characteristics of Polymer–Carbon Composites* (pp. 457–502). https://doi.org/10.1007/978-981-13-2688-2_13

BIS, I. 8112: 2013}. (2013). IS 8112: 2013, Ordinary Portland Cement, 43 grade—Specification, Bureau of Indian Standards. *Bureau of Indian Standards New Delhi, India*.

Chen, Y., Li, X., Dong, B., Du, H., Yan, R., & Wang, L. (2022). High-temperature properties of cement paste with graphene oxide agglomerates. *Construction and Building Materials*, *320*, 126286. doi.org/10.1016/j.conbuildmat.2021.126286

Chintalapudi, K., & Pannem, R. M. R. (2020). An intense review on the performance of Graphene Oxide and reduced Graphene Oxide in an admixed cement system. *Construction and Building Materials*, *259*, 120598. https://doi.org/10.1016/j.conbuildmat.2020.120598

Dai, Y., Sun, M., Liu, C., & Li, Z. (2010). Electromagnetic wave absorbing characteristics of carbon black cement-based composites. *Cement and Concrete Composites*, *32*(7), 508–513. https://doi.org/10.1016/j.cemconcomp.2010.03.009

Donnet, J.-B., Bansal, R. C., & Wang, M.-J. (2018). *Carbon Black* (J.-B. Donnet, Ed.). Routledge. https://doi.org/10.1201/9781315138763

Du, H., & Pang, S. D. (2015). Enhancement of barrier properties of cement mortar with graphene nanoplatelet. *Cement and Concrete Research*, *76*, 10–19. https://doi.org/10.1016/j.cemconres.2015.05.007

Gholampour, A., Valizadeh Kiamahalleh, M., Tran, D. N. H., Ozbakkaloglu, T., & Losic, D. (2017). From Graphene Oxide to Reduced Graphene Oxide: Impact on the Physiochemical and Mechanical Properties of Graphene–Cement Composites. *ACS Applied Materials & Interfaces*, *9*(49), 43275–43286. https://doi.org/10.1021/acsami.7b16736

Guan, X., Bai, S., Li, H., & Ou, J. (2020). Mechanical properties and microstructure of multi-walled carbon nanotube-reinforced cementitious composites under the

early-age freezing conditions. *Construction and Building Materials*, *233*, 117317. https://doi.org/10.1016/j.conbuildmat.2019.117317

Han, S., Hossain, M. S., Ha, T., & Yun, K. K. (2022). Graphene-oxide-reinforced cement composites mechanical and microstructural characteristics at elevated temperatures. *Nanotechnology Reviews*, *11*(1), 3174–3194. https://doi.org/10.1515/ntrev-2022-0495

He, S., Chai, J., Yang, Y., Cao, J., Qin, Y., & Xu, Z. (2023). Effect of nano-reinforcing phase on the early hydration of cement paste: A review. *Construction and Building Materials*, *367*, 130147. doi.org/10.1016/j.conbuildmat.2022.130147

Huang, C., & Cheng, Q. (2017). Learning from nacre: Constructing polymer nanocomposites. *Composites Science and Technology*, *150*, 141–166. https://doi.org/10.1016/j.compscitech.2017.07.021

Huang, J., Rodrigue, D., & Guo, P. (2022). Flexural and compressive strengths of carbon nanotube reinforced cementitious composites as a function of curing time. *Construction and Building Materials*, *318*, 125996. https://doi.org/10.1016/j.conbuildmat.2021.125996

Huang, Y., Li, H., & Qian, S. (2018). Self-sensing properties of Engineered Cementitious Composites. *Construction and Building Materials*, *174*, 253–262. https://doi.org/10.1016/j.conbuildmat.2018.04.129

IS-1963, I. 2386 (Part. (1963). *Recommended guideline for methods of test for fine aggregate for concrete*. Bureau of Indian standards New Delhi.

IS-516-1959,. Methods of tests for strength of concrete. *Bur. Indian Stand.*

Indukuri, C. S. R., & Nerella, R. (2021). Enhanced transport properties of graphene oxide-based cement composite material. *Journal of Building Engineering*, *37*, 102174. https://doi.org/10.1016/j.jobe.2021.102174

Iqbal, H. W., Khushnood, R. A., Latif Baloch, W., Nawaz, A., & Tufail, R. F. (2020). Influence of graphite nano/micro platelets on the residual performance of high strength concrete exposed to elevated temperature. *Construction and Building Materials*, *253*, 119029. https://doi.org/10.1016/j.conbuildmat.2020.119029

Irshidat, M. R., Al-Nuaimi, N., Ahmed, W., & Rabie, M. (2021). Feasibility of recycling waste carbon black in cement mortar production: Environmental life cycle assessment and performance evaluation. *Construction and Building Materials*, *296*, 123740. https://doi.org/10.1016/j.conbuildmat.2021.123740

IS, B. I. S. (1999). 9103: 1999. *Concrete Admixtures-Specification.(First Revision). New Delhi (India): Bureau of Indian Standards*.

IS, I. S. C. (1970). 383. *Specification for Coarse and Fine Aggregates from Natural Sources for Concrete, Bureau of Indian Standards, New Delhi*.

Ismail, F. I., Shafiq, N., Abbas, Y. M., Bheel, N., Benjeddou, O., Ahmad, M., Sabri Sabri, M. M., & Ateya, E. S. (2022). Behavioral assessment of graphene nanoplatelets reinforced concrete beams by experimental, statistical, and analytical methods. *Case Studies in Construction Materials*, *17*, e01676. https://doi.org/10.1016/j.cscm.2022.e01676

Jayachandra, Yashwanth, H. J., Ramalinga Reddy, Y., & Sanjith, J. (2022). Strengthening of Cement mortar by Reinforcing Carbon Based Nano Material. *IOP Conference Series: Materials Science and Engineering*, *1255*(1), 012018. https://doi.org/10.1088/1757-899X/1255/1/012018

Kaushik, B. K., & Majumder, M. K. (2015). *Carbon Nanotube: Properties and Applications* (pp. 17–37). https://doi.org/10.1007/978-81-322-2047-3_2

Kishore, K., Pandey, A., Wagri, N. K., Saxena, A., Patel, J., & Al-Fakih, A. (2023). Technological challenges in nanoparticle-modified geopolymer concrete: A comprehensive review on nanomaterial dispersion, characterization techniques and its mechanical properties. *Case Studies in Construction Materials*, *19*, e02265. https://doi.org/10.1016/j.cscm.2023.e02265

Kong, X., Wang, R., Zhang, T., Sun, R., & Fu, Y. (2022). Effects of graphene oxygen content on durability and microstructure of cement mortar composites. *Construction and Building Materials*, *354*, 129121. https://doi.org/10.1016/j.conbuildmat.2022.129121

Konsta-Gdoutos, M. S., Metaxa, Z. S., & Shah, S. P. (2010). Multi-scale mechanical and fracture characteristics and early-age strain capacity of high performance carbon

nanotube/cement nanocomposites. *Cement and Concrete Composites*, *32*(2), 110–115. https://doi.org/10.1016/j.cemconcomp.2009.10.007

Korayem, A. H., Tourani, N., Zakertabrizi, M., Sabziparvar, A. M., & Duan, W. H. (2017). A review of dispersion of nanoparticles in cementitious matrices: Nanoparticle geometry perspective. *Construction and Building Materials*, *153*, 346–357. https://doi.org/10.1016/j.conbuildmat.2017.06.164

Kostoff, R. N., Koytcheff, R. G., & Lau, C. G. Y. (2007). Global nanotechnology research literature overview. *Technological Forecasting and Social Change*, *74*(9), 1733–1747. https://doi.org/10.1016/j.techfore.2007.04.004

Kumar, H. V., Woltornist, S. J., & Adamson, D. H. (2016). Fractionation and characterization of graphene oxide by oxidation extent through emulsion stabilization. *Carbon*, *98*, 491–495. https://doi.org/10.1016/j.carbon.2015.10.083

Lee, H., Park, S., Kim, D., & Chung, W. (2022). Heating Performance of Cementitious Composites with Carbon-Based Nanomaterials. *Crystals*, *12*(5), 716. https://doi.org/10.3390/cryst12050716

Lee, S.-J., Jeong, S.-H., Kim, D.-U., & Won, J.-P. (2020). Effects of graphene oxide on pore structure and mechanical properties of cementitious composites. *Composite Structures*, *234*, 111709. https://doi.org/10.1016/j.compstruct.2019.111709

Li, X., & Li, M. (2019). Multifunctional self-sensing and ductile cementitious materials. *Cement and Concrete Research*, *123*, 105714. https://doi.org/10.1016/j.cemconres.2019.03.008

Lima, G. E. S. de, Nalon, G. H., Santos, R. F., Ribeiro, J. C. L., Carvalho, J. M. F. de, Pedroti, L. G., & Araújo, E. N. D. de. (2021). Microstructural Investigation of the Effects of Carbon Black Nanoparticles on Hydration Mechanisms, Mechanical and Piezoresistive Properties of Cement Mortars. *Materials Research*, *24*(4). https://doi.org/10.1590/1980-5373-mr-2020-0539

Liu, Q., Wu, W., Xiao, J., Tian, Y., Chen, J., & Singh, A. (2019). Correlation between damage evolution and resistivity reaction of concrete in-filled with graphene nanoplatelets. *Construction and Building Materials*, *208*, 482–491. https://doi.org/10.1016/j.conbuildmat.2019.03.036

Lu, D., Shi, X., & Zhong, J. (2022). Nano-engineering the interfacial transition zone in cement composites with graphene oxide. *Construction and Building Materials*, *356*, 129284. https://doi.org/10.1016/j.conbuildmat.2022.129284

Malik, M., Bhattacharyya, S. K., & Barai, S. V. (2021). Thermal and mechanical properties of concrete and its constituents at elevated temperatures: A review. *Construction and Building Materials*, *270*, 121398. https://doi.org/10.1016/j.conbuildmat.2020.121398

Monteiro, A. O., Cachim, P. B., & Costa, P. M. F. J. (2015). Electrical Properties of Cement-based Composites Containing Carbon Black Particles. *Materials Today: Proceedings*, *2*(1), 193–199. https://doi.org/10.1016/j.matpr.2015.04.021

Moosavi, A., Asadi, S., & Shoraki, H. J. (2019). Microstructure and mechanical properties of tabular alumina composites with geopolymer binder at elevated temperatures. *Ceramics International*, *45*(7), 9092–9098. https://doi.org/10.1016/j.ceramint.2019.01.246

Muradyan, N. G., Gyulasaryan, H., Arzumanyan, A. A., Badalyan, M. M., Kalantaryan, M. A., Vardanyan, Y. V., Laroze, D., Manukyan, A., & Barseghyan, M. G. (2022). The Effect of Multi-Walled Carbon Nanotubes on the Compressive Strength of Cement Mortars. *Coatings*, *12*(12), 1933. https://doi.org/10.3390/coatings12121933

Nalon, G. H., Ribeiro, J. C. L., Araújo, E. N. D. de, Pedroti, L. G., Carvalho, J. M. F. de, Santos, R. F., & Aparecido-Ferreira, A. (2020). Effects of different kinds of carbon black nanoparticles on the piezoresistive and mechanical properties of cement-based composites. *Journal of Building Engineering*, *32*, 101724. https://doi.org/10.1016/j.jobe.2020.101724

Nalon, G. H., Ribeiro, J. C. L., Araújo, E. N. D. de, Pedroti, L. G., Franco de Carvalho, J. M., Santos, R. F., & Oliveira, D. S. de. (2021). Effects of post-fire curing on the mechanical properties of cement composites containing carbon black nanoparticles and multi-walled carbon nanotubes. *Construction and Building Materials*, *310*, 125118. https://doi.org/10.1016/j.conbuildmat.2021.125118

Nalon, G. H., Ribeiro, J. C. L., de Araújo, E. N. D., Pedroti, L. G., de Carvalho, J. M. F., Santos, R. F., & de Oliveira, D. S. (2021). Residual mechanical properties of mortars containing carbon nanomaterials exposed to high temperatures. *Construction and Building Materials*, *275*, 122123. https://doi.org/10.1016/j.conbuildmat.2020.122123

Naresh Kumar, T., Vishnu Vardhan, K., Hari Krishna, M., & Venkata Nagaraja, P. (2021). Effect of graphene oxide on strength properties of cementitious materials: A review. *Materials Today: Proceedings*, *46*, 2157–2160. https://doi.org/10.1016/j.matpr.2021.02.637

Pehlivan, A. O., Sanrı Karapınar, I., Karakuş, S., Özsoy Özbay, A. E., & Yazgan, A. U. (2023). Evaluation of the Microstructure and Mechanical Properties of Biopolymer-Based Cementitious Composites with Silver Nanoparticles. *Journal of Materials in Civil Engineering*, *35*(3). https://doi.org/10.1061/(ASCE)MT.1943-5533.0004650

Peng, H., Ge, Y., Cai, C. S., Zhang, Y., & Liu, Z. (2019). Mechanical properties and microstructure of graphene oxide cement-based composites. *Construction and Building Materials*, *194*, 102–109. https://doi.org/10.1016/j.conbuildmat.2018.10.234

Prabavathy, S., Jeyasubramanian, K., Prasanth, S., Hikku, G. S., & Robert, R. B. J. (2020). Enhancement in behavioral properties of cement mortar cubes admixed with reduced graphene oxide. *Journal of Building Engineering*, *28*, 101082. https://doi.org/10.1016/j.jobe.2019.101082

Pulkit, U., & Adhikary, S. Das. (2022). Effect of micro-structural changes on concrete properties at elevated temperature: Current knowledge and outlook. *Structural Concrete*, *23*(4), 1995–2014. https://doi.org/10.1002/suco.202000365

Qureshi, T. S., & Panesar, D. K. (2019). Impact of graphene oxide and highly reduced graphene oxide on cement-based composites. *Construction and Building Materials*, *206*, 71–83. https://doi.org/10.1016/j.conbuildmat.2019.01.176

Qureshi, T. S., & Panesar, D. K. (2020). Nano reinforced cement paste composite with functionalized graphene and pristine graphene nanoplatelets. *Composites Part B: Engineering*, *197*, 108063. https://doi.org/10.1016/j.compositesb.2020.108063

Ramezani, M., Dehghani, A., & Sherif, M. M. (2022). Carbon nanotube reinforced cementitious composites: A comprehensive review. *Construction and Building Materials*, *315*, 125100. https://doi.org/10.1016/j.conbuildmat.2021.125100

Rathinavel, S., Priyadharshini, K., & Panda, D. (2021). A review on carbon nanotube: An overview of synthesis, properties, functionalization, characterization, and the application. *Materials Science and Engineering: B*, *268*, 115095. https://doi.org/10.1016/j.mseb.2021.115095

Rezania, M., Panahandeh, M., Razavi, N., & Berto, F. (2019). Experimental study of the simultaneous effect of nano-silica and nano-carbon black on permeability and mechanical properties of the concrete. *Theoretical and Applied Fracture Mechanics*, *104*, 102391. https://doi.org/10.1016/j.tafmec.2019.102391

Sedaghatdoost, A., & Behfarnia, K. (2018). Mechanical properties of Portland cement mortar containing multi-walled carbon nanotubes at elevated temperatures. *Construction and Building Materials*, *176*, 482–489. https://doi.org/10.1016/j.conbuildmat.2018.05.095

Sevim, O., Jiang, Z., & Ozbulut, O. E. (2022). Effects of graphene nanoplatelets type on self-sensing properties of cement mortar composites. *Construction and Building Materials*, *359*, 129488. https://doi.org/10.1016/j.conbuildmat.2022.129488

Shamsaei, E., de Souza, F. B., Yao, X., Benhelal, E., Akbari, A., & Duan, W. (2018). Graphene-based nanosheets for stronger and more durable concrete: A review. *Construction and Building Materials*, *183*, 642–660. https://doi.org/10.1016/j.conbuildmat.2018.06.201

Sikora, P., Abd Elrahman, M., Chung, S.-Y., Cendrowski, K., Mijowska, E., & Stephan, D. (2019). Mechanical and microstructural properties of cement pastes containing carbon nanotubes and carbon nanotube-silica core-shell structures, exposed to elevated temperature. *Cement and Concrete Composites*, *95*, 193–204. https://doi.org/10.1016/j.cemconcomp.2018.11.006

Singh, L. P., Ali, D., Tyagi, I., Sharma, U., Singh, R., & Hou, P. (2019). Durability studies of nano-engineered fly ash concrete. *Construction and Building Materials*, *194*, 205–215. https://doi.org/10.1016/j.conbuildmat.2018.11.022

Tao, J., Wang, X., Wang, Z., & Zeng, Q. (2019). Graphene nanoplatelets as an effective additive to tune the microstructures and piezoresistive properties of cement-based composites. *Construction and Building Materials*, *209*, 665–678. https://doi.org/10.1016/j.conbuildmat.2019.03.173

Valizadeh Kiamahalleh, M., Gholampour, A., Tran, D. N. H., Ozbakkaloglu, T., & Losic, D. (2020). Physiochemical and mechanical properties of reduced graphene oxide–cement mortar composites: Effect of reduced graphene oxide particle size. *Construction and Building Materials*, *250*, 118832. https://doi.org/10.1016/j.conbuildmat.2020.118832

Wang, B., & Shuang, D. (2018). Effect of graphene nanoplatelets on the properties, pore structure and microstructure of cement composites. *Materials Express*, *8*(5), 407–416. https://doi.org/10.1166/mex.2018.1447

Yakovlev, A. V., Finaenov, A. I., Zabud'kov, S. L., & Yakovleva, E. V. (2006). Thermally expanded graphite: Synthesis, properties, and prospects for use. *Russian Journal of Applied Chemistry*, *79*(11), 1741–1751. https://doi.org/10.1134/S1070427206110012

Zhai, S., Pang, B., Liu, G., Zhang, Y., Xu, K., She, W., & Zhang, Y. (2021). Investigation on preparation and multifunctionality of reduced graphene oxide cement mortar. *Construction and Building Materials*, *275*, 122119. https://doi.org/10.1016/j.conbuildmat.2020.122119

Zhang, Q., Luan, C., Yu, C., Huang, Y., & Zhou, Z. (2022b). Mechanisms of carbon black in multifunctional cement matrix: Hydration and microstructure perspectives. *Construction and Building Materials*, *346*, 128455. https://doi.org/10.1016/j.conbuildmat.2022.128455

Zhao, L., Guo, X., Song, L., Song, Y., Dai, G., & Liu, J. (2020). An intensive review on the role of graphene oxide in cement-based materials. *Construction and Building Materials, 241*, 117939. https://doi.org/10.1016/j.conbuildmat.2019.117939

Document Information

Analyzed document	Nitish-802124012.pdf (D172445637)
Submitted	7/29/2023 1:20:00 PM
Submitted by	Danie Roy A B
Submitter email	abdanie@thapar.edu
Similarity	4%
Analysis address	abdanie.thapar@analysis.urkund.com

Sources included in the report

SA	**Thesis_Bhaveshpatel.docx** Document Thesis_Bhaveshpatel.docx (D29312710)	1
SA	**MTS - AIP - Full Paper (Revised2).pdf** Document MTS - AIP - Full Paper (Revised2).pdf (D108713369)	1
SA	**Group 5.pdf** Document Group 5.pdf (D111129529)	1
W	URL: https://www.researchgate.net/publication/273311680_Reinforcing_Effects_of_Graphene_Oxide_on_Po... Fetched: 10/30/2019 11:06:17 AM	1
SA	**Thesis main text.pdf** Document Thesis main text.pdf (D170465009)	2
SA	**paper draft.docx** Document paper draft.docx (D110853102)	3
SA	**final+research+report.pdf** Document final+research+report.pdf (D113886318)	1
W	URL: https://www.researchgate.net/publication/299494707_Influence_of_2D_rGO_nanosheets_on_the_prope... Fetched: 11/29/2022 12:57:11 PM	3
W	URL: http://www.revistageintec.net/index.php/revista/article/view/1924/1249 Fetched: 9/30/2021 3:52:46 PM	5
W	URL: https://www.researchgate.net/publication/318593023_A_Critical_Review_on_Research_Progress_of_G... Fetched: 3/23/2023 2:04:00 AM	3
SA	**Effect of Graphene oxide on Portland Cement Composites and its Strength Properties.docx** Document Effect of Graphene oxide on Portland Cement Composites and its Strength Properties.docx (D164416667)	4
W	URL: https://www.degruyter.com/document/doi/10.1515/ntrev-2020-0011/html?lang=en Fetched: 5/19/2022 8:49:14 AM	2
W	URL: https://www.mdpi.com/1996-1944/13/1/230/htm Fetched: 7/29/2021 6:44:04 PM	3
SA	**CBM.pdf** Document CBM.pdf (D55768290)	1